CERTIFICATION OF APPROVAL

# GENERAL GEOLOGY OF PULAU LANGGUN, LANGKAWI, KEDAH AND A PRELIMINARY STUDY ON THE MORPHOLOGY OF GRAPTOLITES

By

Johan Bin Zainal Abidin

13830

A project dissertation submitted to the

Petroleum Geoscience Programme

Universiti Teknologi PETRONAS

in a partial fulfillment of the requirement for the

Bachelor of Technology (Hons)

(Petroleum Geoscience)

Approved by,

_________________________________

(DR SUHAILI BIN ISMAIL)

UNIVERSITI TEKNOLOGI PETRONAS

TRONOH, PERAK

MAY 2014

CERTIFICATION OF ORIGINALITY

This is to certify that I am responsible for the work submitted in this project, that the original work is my own except as specified in the references and acknowledgements, and that the original work contained herein have not been undertaken or done by unspecified sources or persons.

JOHAN BIN ZAINAL ABIDIN

# ABSTRACT

The geology of northeastern Pulau Langgun was found to consist of shale interbedded with carbonaceous mudstone, dark-colored limestone, mudstone, and siltstone with sandstone lenses, which is in respect with its geologic age, being from Ordovician to Carboniferous in age. This is in accordance to the sequence developed in previous study, Tanjong Dendang Formation, Mempelam Limestone, Timah Tasoh Formation, and Langgun Red Beds (Basal Singa Formation). Structurally, the outcrops of Pulau Langgun are not exempted from the tectonic forces exerted on the Langkawi islands, which is trending ENE-WSW. Among the structures observed include conjugate joints, orthogonal joints, a normal fault and folds. Known for its abundance of fossils, particularly graptolites, samples were taken from the Tanjong Dendang Formation to be observed under the binocular microscope. Sketches of the fossils indicate that the graptolites discovered are of *Glyptograptus* sp., *Dimorphograptus* sp., & *Pristiograptus* sp. which originate from the lower Silurian. The Total Carbon Analysis shows that the organic carbon content of the outcrops here are of poor to very good, which may suggest the rock potential as source rock. This will enhance the source rock studies of Paleozoic rocks in Malaysia in future oil and gas explorations of the area.

# ACKNOWLEDGEMENT

First of all, I would like to thank my Final Year Project supervisor, Dr. Suhaili Bin Ismail for all his assistance and sharing his knowledge upon the topic of my project in completing this project throughout the entire length of this project.

I also would like to thank my parents, all lecturers and friends who has been very supportive in this 5 years of my study in Universiti Teknologi PETRONAS. The final year project is a great exposure for me as a Petroleum Geoscience student, at which the project helps us to implement and to test theories learnt in classroom into practice, thus securing the knowledge to ourselves. In the project titled "General Geology of Pulau Langgun, Langkawi, Kedah with Emphasis on the Morphological Studies of Graptolites", I have learned a lot in conducting a geological fieldwork as well as conducting a number of tests to confirm the ideas and hypotheses based on the observations of the study area. It is also hoped that the project can be used and useful to the geological community today.

Next, I also would like to acknowledge all the personnel who at which has helped me in completing this project directly or indirectly. Special thanks to the laboratory technicians of Universiti Teknologi PETRONAS and not to forget the staff of Jabatan Mineral dan Geosains, Ipoh for the guidance given.

# TABLE OF CONTENTS

# LIST OF FIGURES

## LIST OF TABLES



## LIST OF APPENDICES

# CHAPTER 1

# INTRODUCTION

## 1. INTRODUCTION

### 1.1. Background

Pulau Langgun is one of the many islands in Langkawi, Kedah situated in the Northwestern Domain of the Malaysian Western Belt. It is located in the northeast part of the main island, close to the Malaysian-Thailand border (Figure 1).

Pulau Langgun is uninhabited. Geologically, Pulau Langgun is made up of mainly the Setul Group and the Singa Formation (Gobbett & Hutchison, 1973; Jones, 1976; Lee, 2009). The Setul Group is made up of Timah Tasoh Formation, which is mainly shale and siltstone, Mempelam Limestone, Tanjong Dendang Formation, which is mainly shale, and Kaki Bukit Limestone, while the Singa Formation is mainly mudstone and quartzite.

The island of Pulau Langgun has been the center for a lot of fossil discovery for Malaysia, even introducing to the world species of fossils that are native to Malaysia. Among the fossils discovered in Pulau Langgun, the graptolites have been the most significant.


Figure 1: Location of Pulau Langgun

According to Benton & Harper (2009), graptolites are stick-like fossils found mostly in Lower Paleozoic formations and was used as an index fossil in biostratigraphy due to its prominence in the Lower Paleozoic strata (Figure 2). The graptolites are largely isolated towards the Ordovician and Silurian biozones thus making it in accordance with the presence of outcrops in Pulau Langgun, which is mostly Ordovician and Silurian in age.

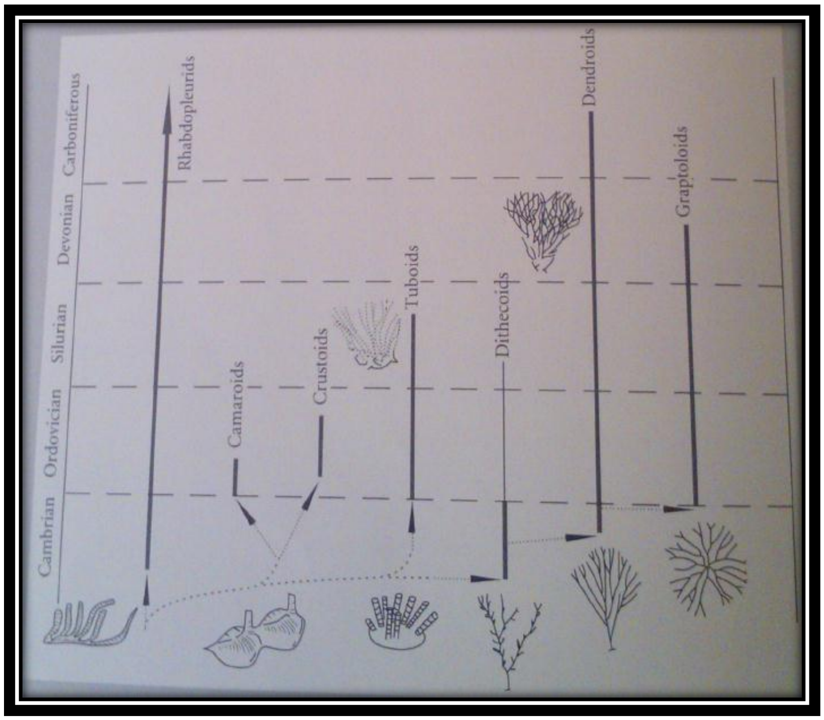


Figure 2: Historical distribution of graptolites in the geologic timeline (Benton & Harper, 2009, p. 414)

Apart from the rock formations, Pulau Langgun also has an occurrence of graptolites, which was discovered by Jones (1976). Since Jones, no study has been carried out on the graptolite occurrence in Pulau Langgun.

### 1.2. Problem Statement

There have been several studies done on the geology of Pulau Langgun (Jones, 1976; Lee, 2009). The geology of Pulau Langgun has been of interest for years, with the most recent study by Lee, who proposed renaming the rock formations on Pulau Langgun previously named by Jones (1976), which has intrigued an explanation for the necessity of the renaming. This research is reviewing the general geology of Pulau Langgun, which also include study on the morphology of graptolites found in the area. Most of the study works on the general geology aspect.


Figure 3: Teluk Mempelam and associated lithology (Gobbett & Hutchison, 1973, p. 44)

## 1.3. Objectives of Study

### 1.3.1. General Objective

The general objective of this research is to study the general geology of the northern Pulau Langgun in detail, which includes the analysis of the structural trend of the area, sedimentology, palaeontology, and the petrographic study of the rocks.

### 1.3.2. Specific Objective

The specific objectives are as follows:

- To map and produce a geological map of northern Pulau Langgun area.
- To study the morphology of the graptolites in Pulau Langgun area.
- To examine the source rock potential of formations in Pulau Langgun area.

## 1.4. Scope of Study

The research will be focusing mainly on northern Pulau Langgun. It will not cover the other parts of Langkawi islands. Special interest will be on the morphological studies of the graptolites. General geology will cover all rock irrespective of age.

# CHAPTER 2

# LITERATURE REVIEW

## 2. LITERATURE REVIEW

### 2.1. General Geology

Pulau Langgun comprises mainly rocks of the Paleozoic era. The rock formations found on the island are the Setul Formation and the Singa Formation (Gobbett & Hutchison, 1973; Jones, 1976). Outcrops of the two formations can be found along the shore.

The Setul Formation made up the majority of the geology of Pulau Langgun. The Setul Formation is mainly dark-colored limestone, which is crystalline and impure due to its argillaceous nature, interbedded with two detrital members, namely Upper Detrital Member and Lower Detrital Member. The limestone is mostly nodular and stylolitic (Jones, 1976). The Lower Detrital Member includes black carbonaceous siltstone, flaggy shale, and chert. The units of the Lower Detrital Member are described in Table 1.

Table 1: The breakdown of the units of the Lower Detrital Member

| Unit | Description |
|---|---|
| 8 | Bedded Setul Limestone |
| 7 | Black, carbonaceous siltstone and fissile shale with abundant graptolites |
| 6 | Closely bedded, black carbonaceous and siliceous shale and chert without macrofossils |
| 5 | Black carbonaceous and cherty mudstone with occasional very fragmentary graptolites |
| 4 | Closely bedded, carbonaceous quartzite and siltstone, veined by quartz stringers |
| 3 | Thickly bedded, carbonaceous siltstone and gritty subgreywacke with shelly fossils |
| 2 | Well-bedded, carbonaceous siltstone with abundant graptolites |
| 1 | Bedded Setul Limestone |

According to Gobbett & Hutchison (1973), the Upper Detrital Member comprises contorted reddish-grey to grey mudstone, siltstone and quartzite due to the fact that the Upper Detrital Member is slightly-to-not metamorphosed which is different from the Setul Formation found in other areas besides Pulau Langgun, as explained by Jones (1976). As mentioned by Jones (1976), this is due to the fact that Pulau Langgun is situated away from the tectonic activities and thus are unaffected by the regional metamorphism. The Singa Formation comprises of red conglomeratic mudstone and light to grey quartzite and flaggy shale which overlies unconformably on the Upper Detrital Member of the Setul Formation (Jones, 1976). The units of the Upper Detrital Member and Singa Formation are vividly displayed in Table 2.

Table 2: The breakdown of the units of the Upper Detrital Member and Singa Formation

| Unit | Description |
|---|---|
| 4 | Fossiliferous Upper Devonian conglomeratic mudstone forming the basal beds of the Singa Formation |
| Unconformity | |
| 3 | Strongly contorted brown and grey shale, siltstone, subgreywacke, and orthoquartzite |
| 2 | Fossiliferous dark grey and red bedded mudstone and shale |
| 1 | Bedded Setul Limestone |

The geology of Pulau Langgun is later revised by Lee (2009), best displayed in Figure 4, who says that the southernmost part of Teluk Mempelam is represented by faulted strata of the upper Kaki Bukit Formation and overlying Tanjong Dendang Formation. The upper Kaki Bukit Limestone is mainly thickly-bedded grey limestone. Fossils are abundant and include rare orthocerids, Early Ordovician gastropods including Teiichispira, stromatoporoids, brachiopods and crinoids. The Kaki Bukit Limestone is interpreted to be in peritidal carbonates, possibly deepening to more subtidal conditions in the upper part with evidence of the diverse trilobite fauna, containing 15 Late Ordovician taxa (Kobayashi & Hamada, 1978; Wyatt, Stait, & Burrett, 1983).

The Tanjong Dendang Formation is exposed as two repeating bands, faulted between Kaki Bukit Limestone, in the southern end of Teluk Mempelam. The lithology of the unit varies from quartzite to dark shale and chert. Fossils are abundant in the flaggy shale, including graptolites and trilobites. Jones (1973) recorded graptolites from the unit, indicating an age range from Ordovician to Silurian for the Tanjong Dendang Formation (Cocks, Fortey, & Lee, 2005).

North of the Tanjong Dendang Formation are outcrops and boulders of the overlying Mempelam Limestone. It is mainly composed of bedded stylolitic limestone, although the topmost beds are composed of nodular limestone interbedded with thin black shale. Beds of the uppermost Mempelam Limestone gradually pass upward into black shale of the Timah Tasoh Formation.

According to Meor Hakif Amir Hassan (2013), the Timah Tasoh Formation is overlain by folded and foliated flaggy rock and quartzite. The age of the rocks is uncertain. They may either represent basal beds of the Kubang Pasu Formation, or even possibly Late Devonian strata.

Overlying the folded strata are red mudstone and interbedded quartzite of the Langgun Red Beds, Singa Formation. The Langgun Red Beds are age equivalent to the Chepor Member of the Kubang Pasu Formation in mainland Perlis. Both units share the same facies characteristics and the same fossil assemblage. The fossils and correlation with the Chepor Member indicate an Early Carboniferous age. The Teluk Mempelam exposure ends in the north with a steep limestone cliff, which is upthrusted Kaki Bukit Limestone.

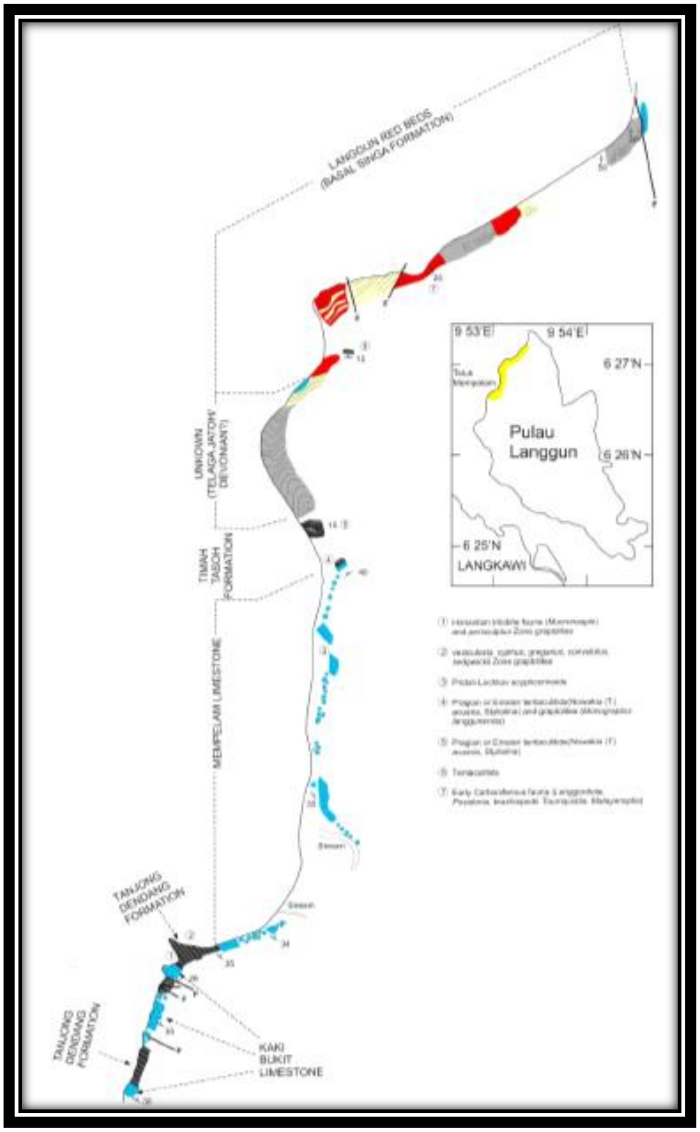


Figure 4: Lee’s (2009) interpretation of Teluk Mempelam. (Hassan, 2013, p. 25)

Jones (1976) interpretation of the stratigraphy of Pulau Langgun is somehow correlatable with Lee (2009) interpretation (Figure 5).

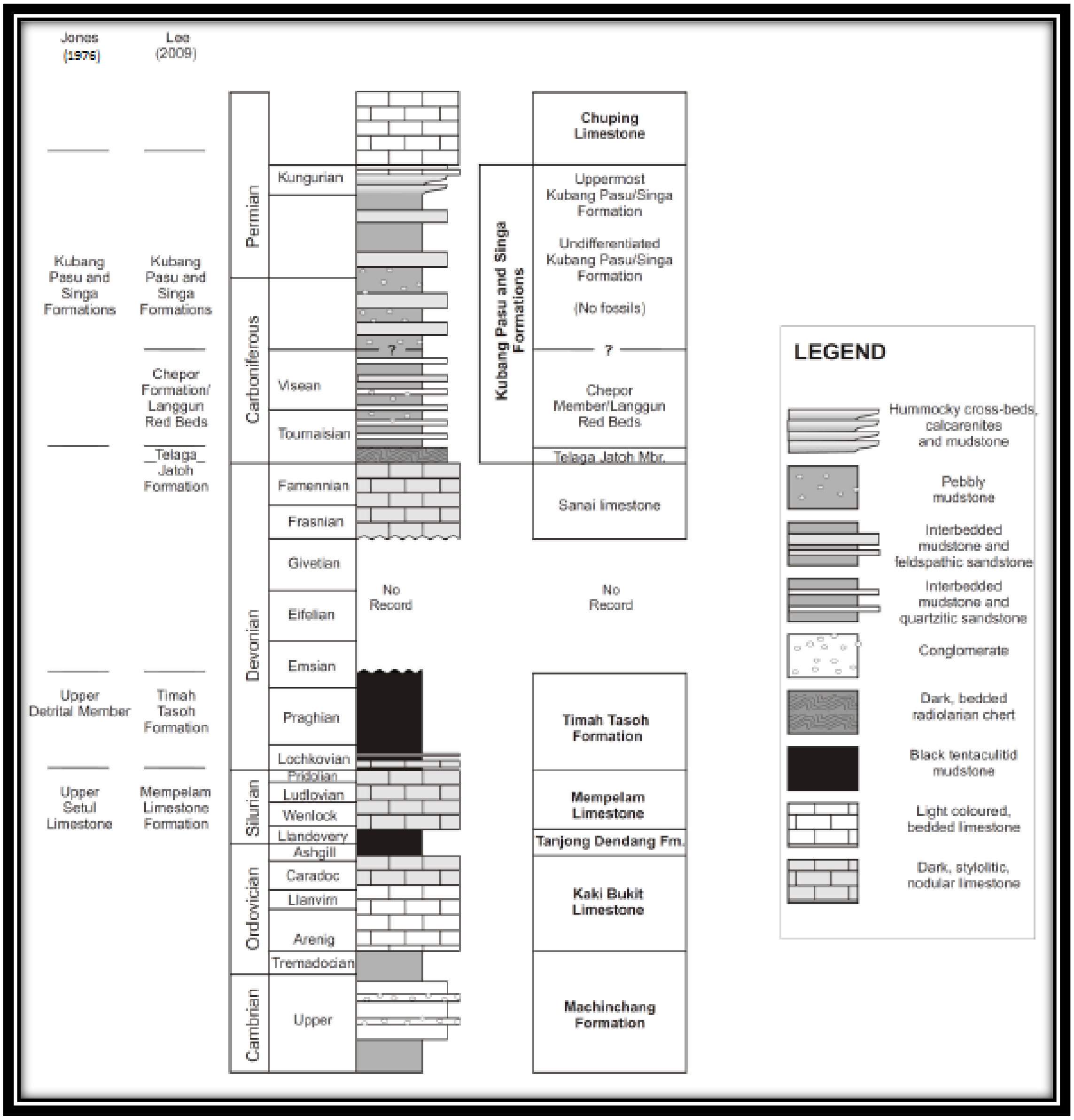


Figure 5: Pulau Langgun's stratigraphy based on Jones (1976) & Lee (2009) (Modified from Meor Hakif Amir Hassan, 2013, p. 5)

## 2.2. Structural Geology

Pulau Langgun has been identified to have situated away from the heavy tectonic activities of the Langkawi Islands (Gobbett & Hutchison, 1973), with the most prominent effect being the Kisap Thrust, which practically divides the Langkawi Islands into 2 zones. However, this statement is countered by Jones (1976) who had discovered an isolated fault on Pulau Langgun trending NE-SW with a dipping of apparently SE-NW (Figure 6 & Figure 7). There is also a freshwater-filled sinkhole in the middle of the island, which is believed to be associated with the fault (Hassan, 2013). In terms of the strata, the beds strike mainly SE-NW with a dipping of NE-SW.


Figure 6: Structural map around Langkawi Islands (Gobbett & Hutchison, 1973)

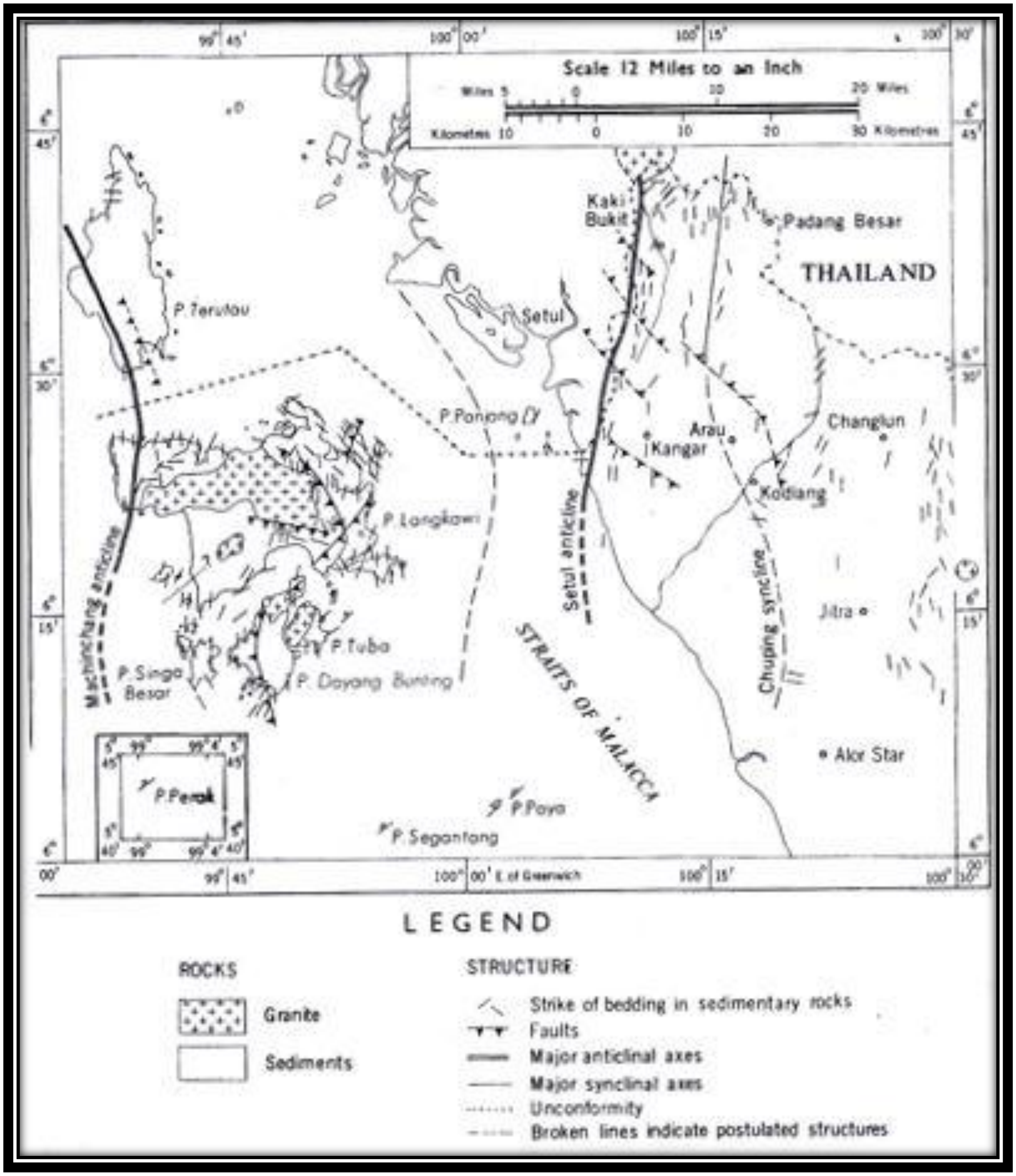


Figure 7: Structural map around Langkawi Islands (Jones, 1976)

# CHAPTER 3

# METHODOLOGY

## 3. METHODOLOGY

This project is divided in two parts, namely, general geology and the preliminary study on the morphology of graptolites in Pulau Langgun.

### 3.1. General Geology of Pulau Langgun

#### 3.1.1. Fieldwork

The basic techniques used for geological mapping studies were used, in addition to other approaches. Two field trips to the area of interest have been conducted, where shore traversing was executed. During this field trip, there is utilization of:

- Geological hammers (for extracting samples of the outcrop);
- Compass (for orienteering and calculating the dip and strike of the outcrop);
- Vinegar (for testing the carbonates);
- Lens (for identifying the size and type of the grains found in the outcrop), and;
- A global positioning system (GPS) device (for orienteering).

### 3.1.2. Post-Fieldwork

The data of the strike and dip of the outcrop collected were plotted on a rose diagram and stereonet diagram to estimate the structural trend of the area. The samples collected were made into thin sections to identify the mineralogy of the rocks. Other analyses include:

- X-Ray Fluorescence (XRF) to qualitatively establish the elemental composition of the samples and to quantitatively measure the concentration of these elements;
- Total Carbon Analysis (TCA) to analyze the carbon content (organic and inorganic) of the sample.

## 3.2. Graptolites Morphology

There are 4 samples, 3 of which are from the previous works obtained from Jabatan Mineral dan Geosains (JMG) and 1 is a fresh sample obtained from study area, have been observed under the binocular microscope and the fossils are subsequently sketched.

# CHAPTER 4

# RESULTS AND DISCUSSION

## 4. RESULTS AND DISCUSSION

### 4.1. Description of Outcrops

#### 4.1.1. Teluk Mempelam

Teluk Mempelam on the northwestern side of the island is unique in that you can walk through the whole Ordovician-Carboniferous geologic record, from older rocks in the south to younger rocks in the north. Generally the strata moderately dip ENE.

Figure 8: Landscape of Teluk Mempelam

**Outcrops 1 – 4**

The lithology of the rock here is found to be carbonate as it reacts with the vinegar for acid tests. The colour is mostly greyish white (Figure 9 - Figure 14)  with yellowish white mineral-like infill, believed to be calcite as it does not scratch the steel file used for the hardness scale test, instead the mineral is scratched. The rocks found in outcrops 3 and 4 are found to be flaky with clays found interbedded within the rock, while there are some of the rock to seem to have a foliated nature. This further confirms the argillaceous nature of the rock (Figure 9) and the possibility that it is mildly metamorphosed.

The outcrop here is believed to be dark, massive and impure limestone with intrusions of crystalline calcite. Such description corresponds with the Setul Formation described by Jones (1976) and with the Mempelam Limestone as described by Lee (2009).

There is also several limestone sea stacks observed throughout the shore of Teluk Mempelam all through outcrops 1 – 4 (Figure 10). Sea stacks are formed over time due to erosion by wind and water, processes of coastal geomorphology. The formation process usually begins when the sea attacks small cracks in a headland and opens them. The cracks then gradually get larger and turn into a small cave. When the cave wears through the headland, an arch forms. Further erosion causes the arch to collapse, leaving the pillar of hard rock standing away from the coast - the stack. Eventually, erosion will cause the stack to collapse, leaving a stump. This stump usually forms a small rock island, low enough for a high tide to submerge (Figure 15).

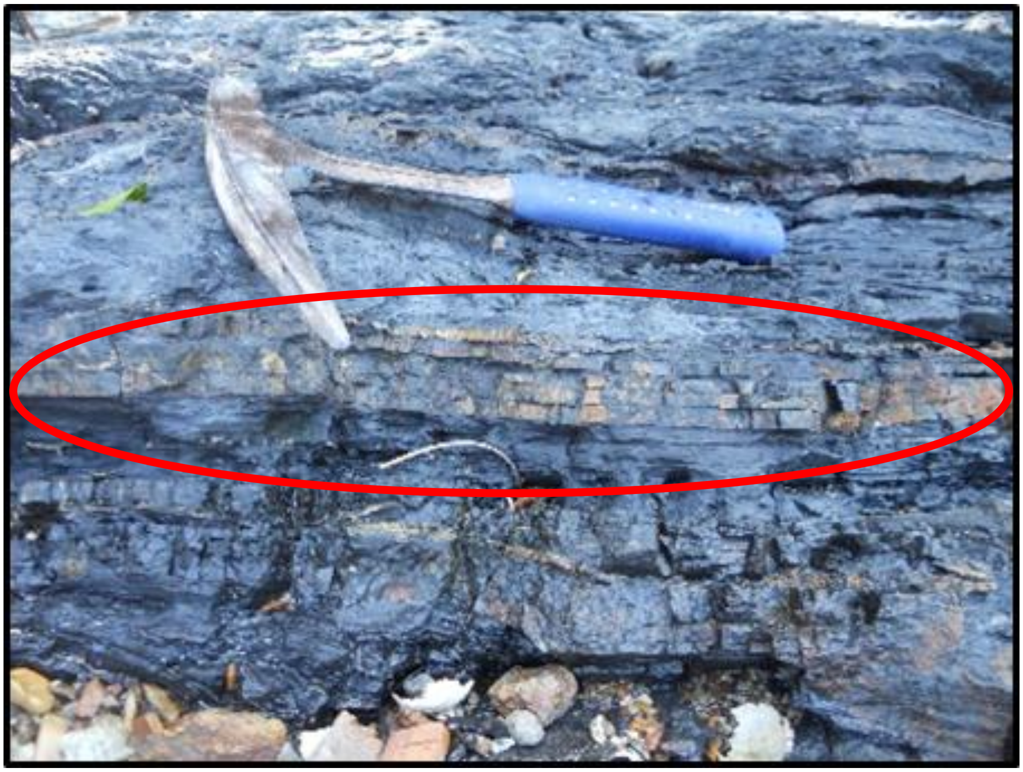

Figure 9: Foliation within parts of the outcrop

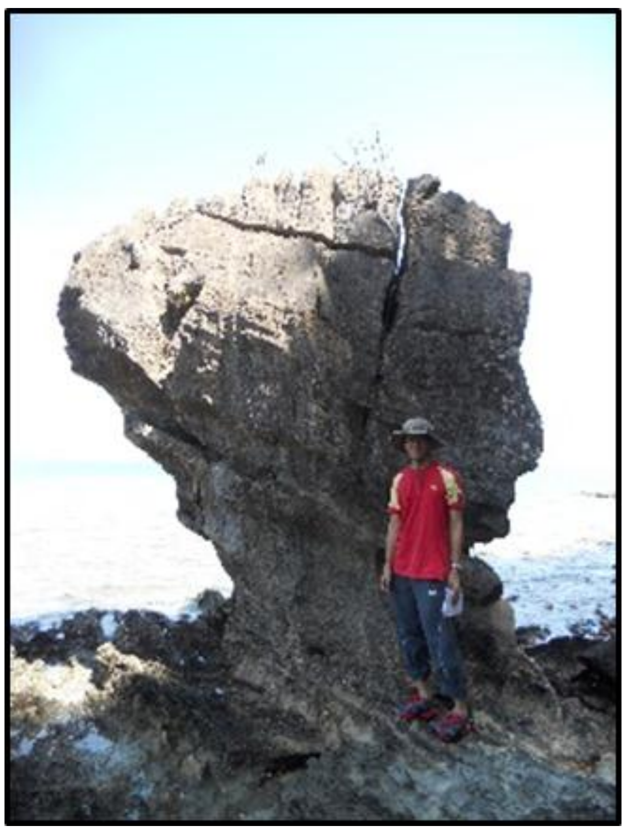

Figure 10: Limestone sea stack in Teluk Mempelam

Figure 11: Exposed greyish white limestone in Teluk Mempelam

Figure 12: Yellowish-white calcite infill.

Figure 13: Massive nature of the outcrops

Figure 14: Massive nature of the outcrops with visible bedding.

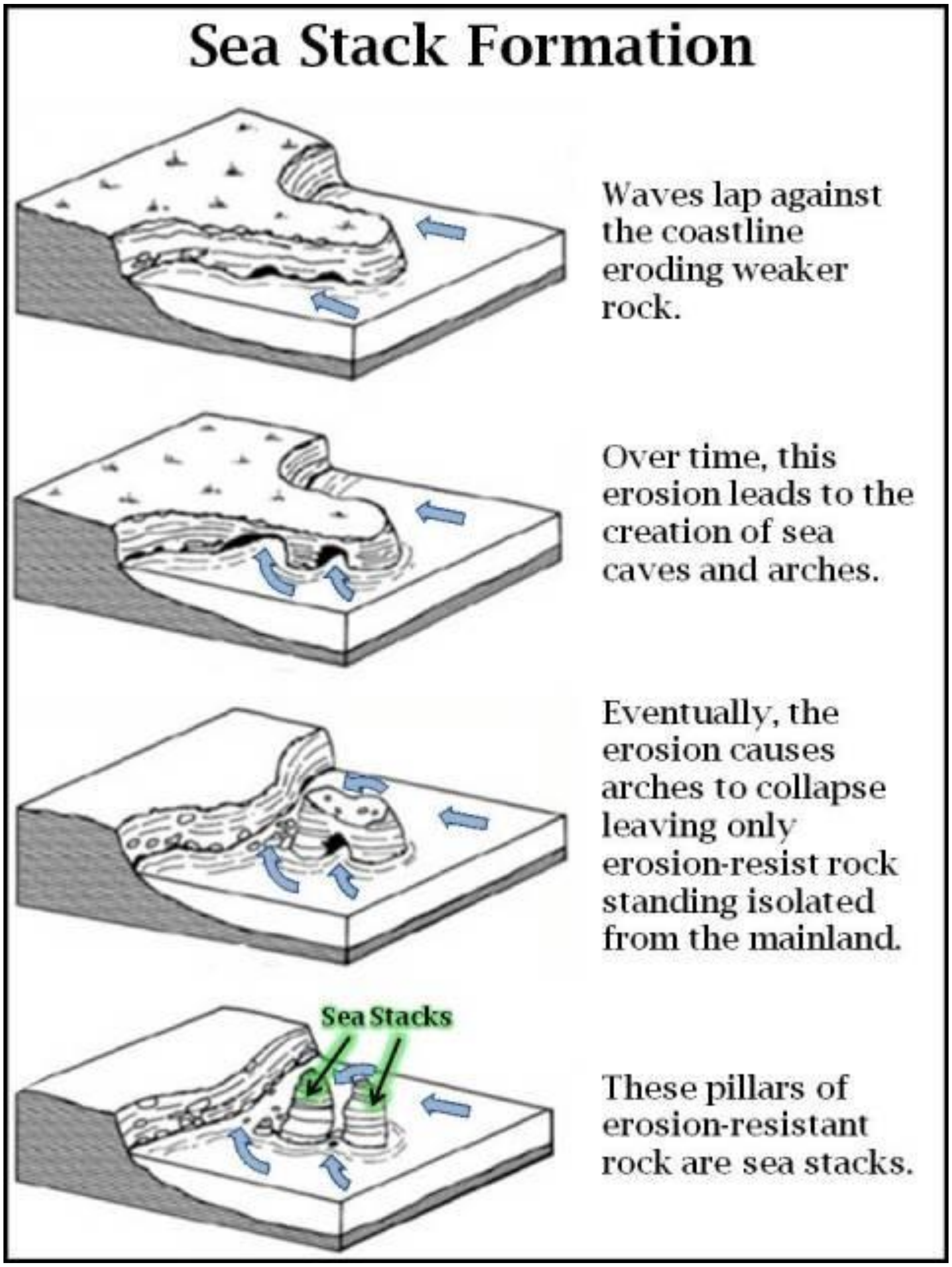


Figure 15: Sea stack formation (Wicander & Monroe, 2009)

**Outcrop 5**

The rock here is seen to be highly fractured and to have a reddish-yellow colour. The fractures are observed to have been infilled by iron oxide due to the rusty nature of the mineral and also its reddish colour (Figure 16).

The rock is observed to be fine-grained as the grains are not felt by hand, which leads it to be regarded as siltstone. This is also due to the rock not having any reaction with the vinegar used for in-situ acid test. Lens within the rock are also observed, where the grains in the lens are seen to be coarse-grained (Figure 17).

The outcrop here is believed to be reddish-yellow siltstone with lenses of sandstone. This is found to correspond with the Upper Detrital Member described by Jones (1976) and with the Timah Tasoh Formation as described by Lee (2009).

Figure 16: The conjugate joints found on the rock with iron oxide infill.

Figure 17: Lens present in the rock.

**Outcrop 6**

The rock is seen to be highly fractured and to have alternating laminations of dark and reddish-yellow colour (Figure 18 – Figure 19). The fractures are observed to have been infilled by iron oxide due to the rusty nature of the mineral and also its reddish colour (Figure 18).

The rock is observed to be fine-grained as the grains are not felt by hand. The rock is found not to be limestone due to the fact that it does not have any reaction with the vinegar used for the in-situ acid test. In Figure 19, an anticline-like structure can be observed from the surface. This leads to the belief that the rock is subjected to folding after its deposition negating the rock from any brittle nature.

The outcrop here is believed to be highly fractured elastic siltstone. This is found to correspond with the Singa Formation found on Teluk Mempelam as described by Jones 1976) and with the Langgun Red Beds (Basal Singa Formation) as described by Lee (2009).

Figure 18: The conjugate joints found on the rock with iron oxide infill.

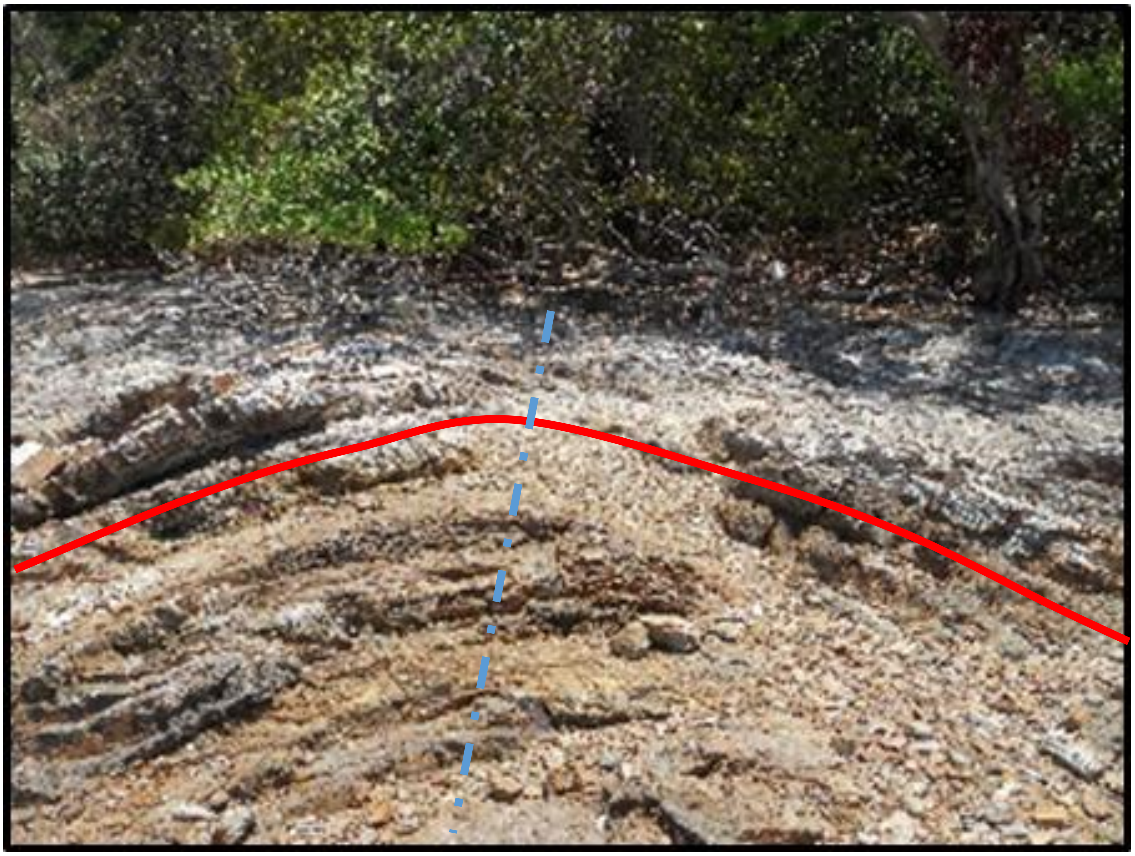

Figure 19: Anticlinal structure (highlighted by the red line) with the dashed blue line being the apex.

**Outcrop 7**

The rock is seen to be flaky and to have a black colour (Figure 20 – Figure 23). The contact between the limestone and the black colour rock here can also be observed (Figure 20).

The rock is observed to be fine-grained as the grains are not felt by hand. The rock is found not to be limestone due to the fact that it does not have any reaction with the vinegar used for in-situ acid test. In Figure 21, Figure 22 & Figure 23, the rock is seen to have fractures and a white-coloured infill can also be observed. The rocks found in outcrops 7 are found to be flaky with clays found interbedded within the rock, while there are some of the rock to seem to have a foliated nature (Figure 20, Figure 22 & Figure 23). This further confirms the argillaceous nature of the rock and the possibility that it is mildly metamorphosed.

The outcrop here is believed to flaky shale interbedded with carbonaceous mudstone. This is found to correspond with the Lower Detrital Member described by Jones (1976) and with the Tanjong Dendang Formation as described by Lee (2009).

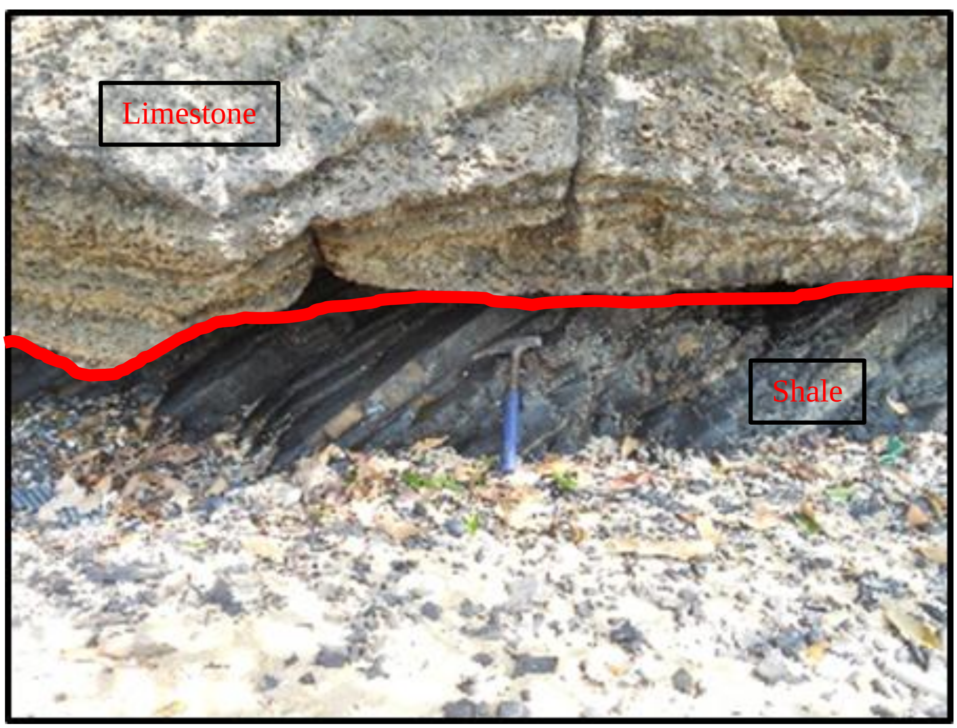


Figure 20: Contact between lime stone and shale (Red colour line). Also note the foliated nature of the shale.

Figure 21: White-coloured infill found on the rock.

Figure 22: White-coloured infill found on the rock.

Figure 23: White-coloured infill found on the rock.

## 4.2. Map

### 4.2.1. Geological Map

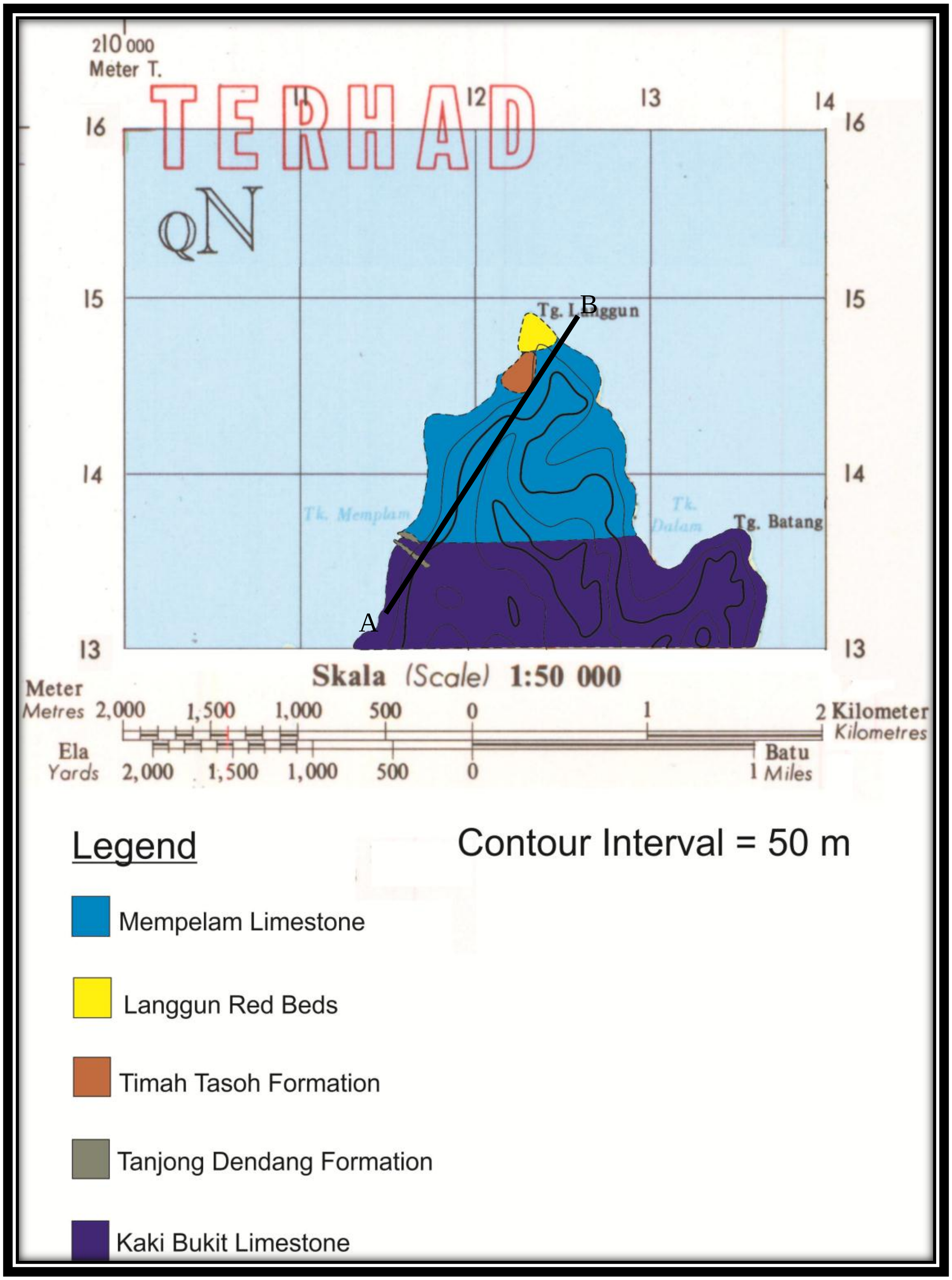


Figure 24: Produced geological map of Teluk Mempelam

### 4.2.2. Geological Cross Section

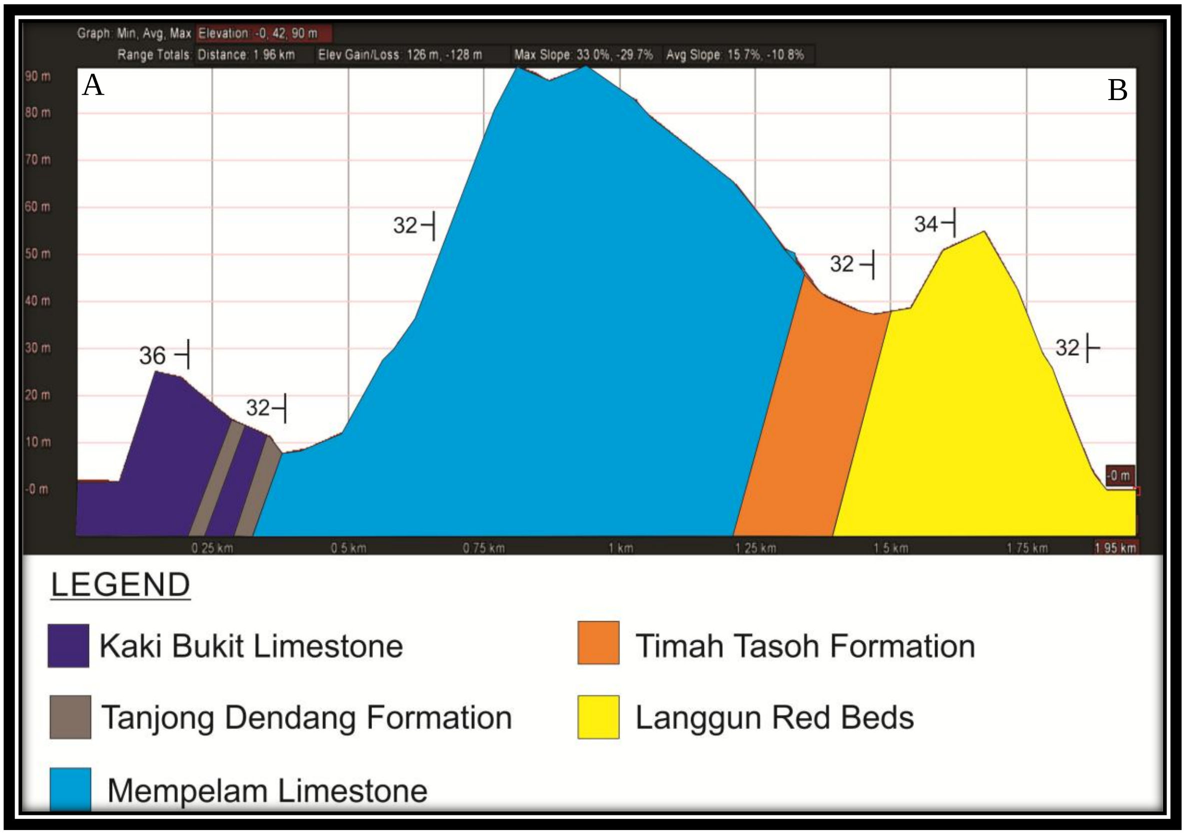


Figure 25: Produced geological cross section of Teluk Mempelam

### 4.3. Structural Geology

The island of Pulau Langgun was observed to be affected by forces as it is observed to be filled with numerous sets of joints. Besides that, there is also a normal fault observed at the northern part of Teluk Mempelam, which indicate the brittle nature of the outcrops. These are normal attributes to exposed rocks or outcrops because of its brittle nature.

Figure 26: The normal fault found, indicated by the red line, on Pulau Langgun. The arrow emphasized the displacement of the block.

The sets of joints observed on the outcrops are mainly conjugate joints, with occasional findings of orthogonal joints. There are also findings of tension gashes on the outcrops. The open fractures are seen to be in the form of lenses. The open fractures are usually infilled by coarse-grained sandstone.

Figure 27: Open fractures, or tension gashes, infilled by coarse-grained sandstone found on outcrop 5.

The joints in the clastics found here are usually infilled by red minerals presumed to be iron oxide due to the heavy weathering by oxidation of the clastics in the area. The carbonates of the area are also heavily jointed with the joints are infilled with white minerals presumed to be calcite. Besides that, it would be interesting to note that the sets of joints of black shale found here are also infilled with the white minerals.

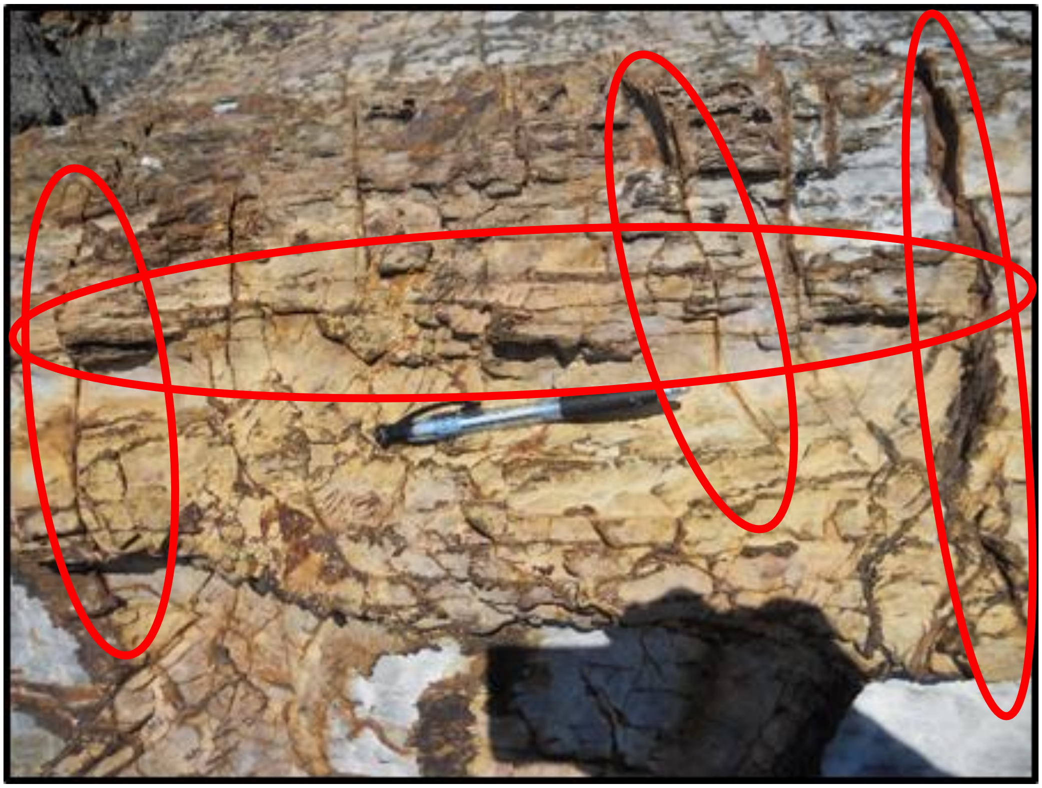

Figure 28: Conjugate joints with iron oxide infill found on the sandstone of outcrop 5.

Figure 29: Yellowish-white calcite infill found in the limestone of outcrop 4.

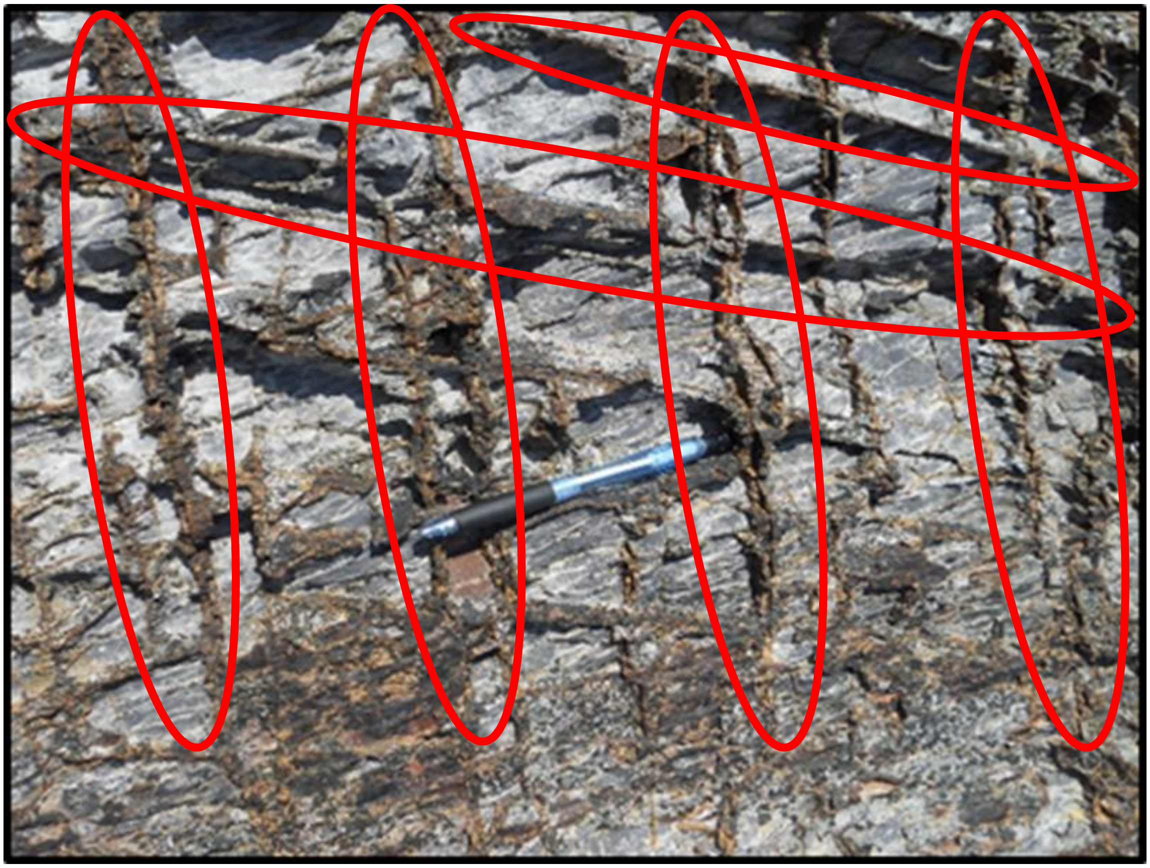

Figure 30: Conjugate joints with iron oxide infill found on the sandstone of outcrop 6.

Figure 31: Conjugate joints infill with quartz found on the shale of outcrop 7.

Figure 32: Conjugate joints infill with quartz found on the shale of outcrop 7.

The readings of the strike and the dipping of the fractures found here are collected and are evaluated using stereonet projection and rose diagram to determine the orientation of the primary forces, $\sigma_1$, and also the minor forces, $\sigma_3$.

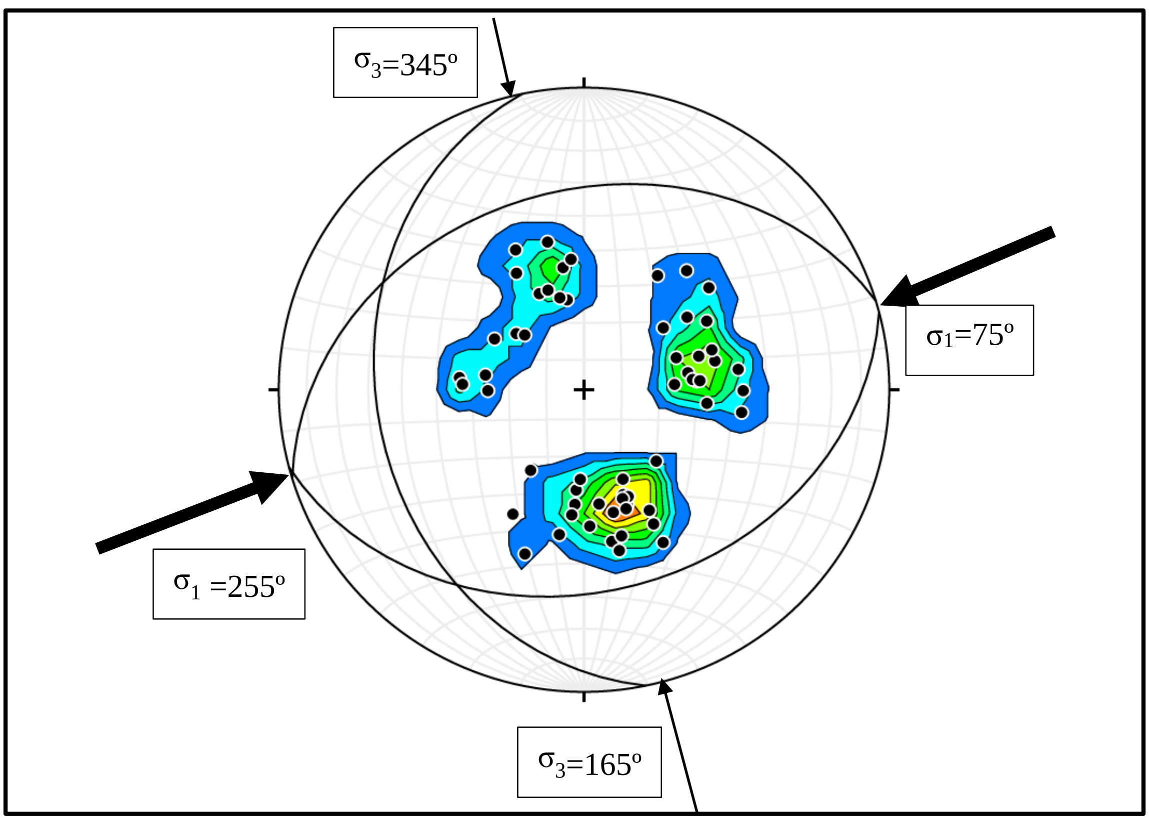


Figure 33: Stereonet projection done based on the readings of the fractures in Teluk Mempelam

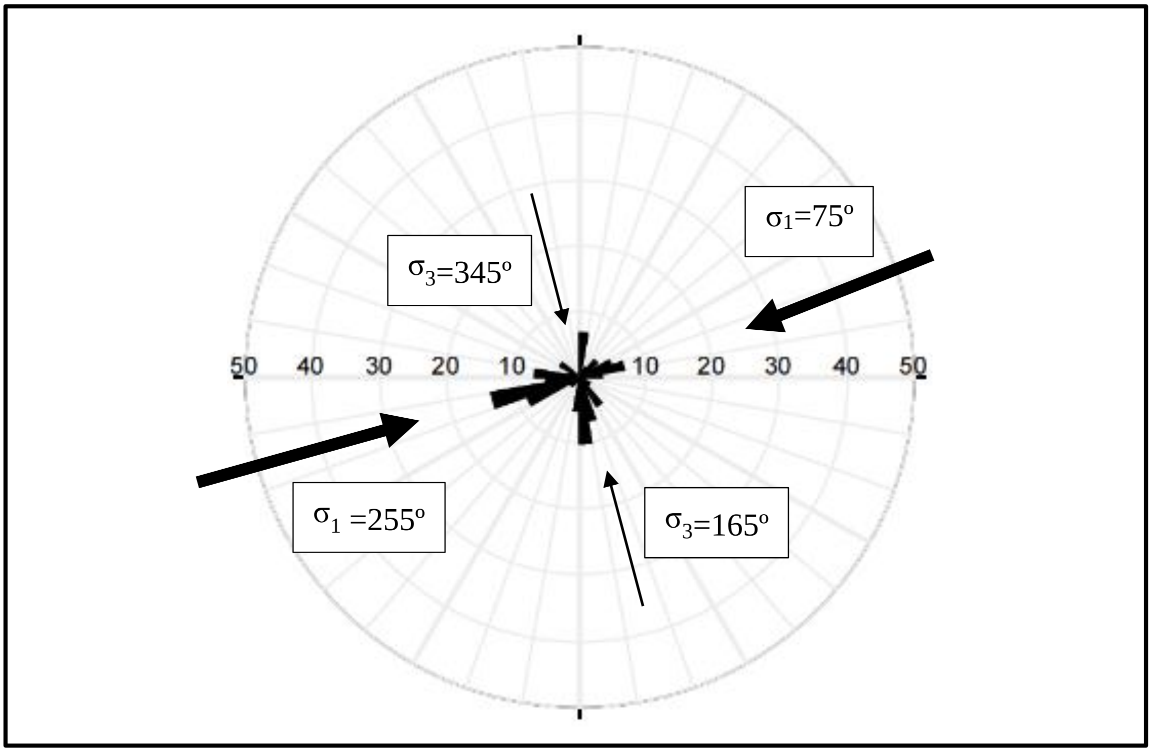


Figure 34: Rose diagram done based on the readings of the fractures in Teluk Mempelam

Comparing both stereonet and rose diagram, it is seen that the outcrops in Teluk Mempelam are subjected to a major stress, $\sigma 1$, of 255º and a minor stress, $\sigma 3$, of 165º.

## 4.4. Sedimentology

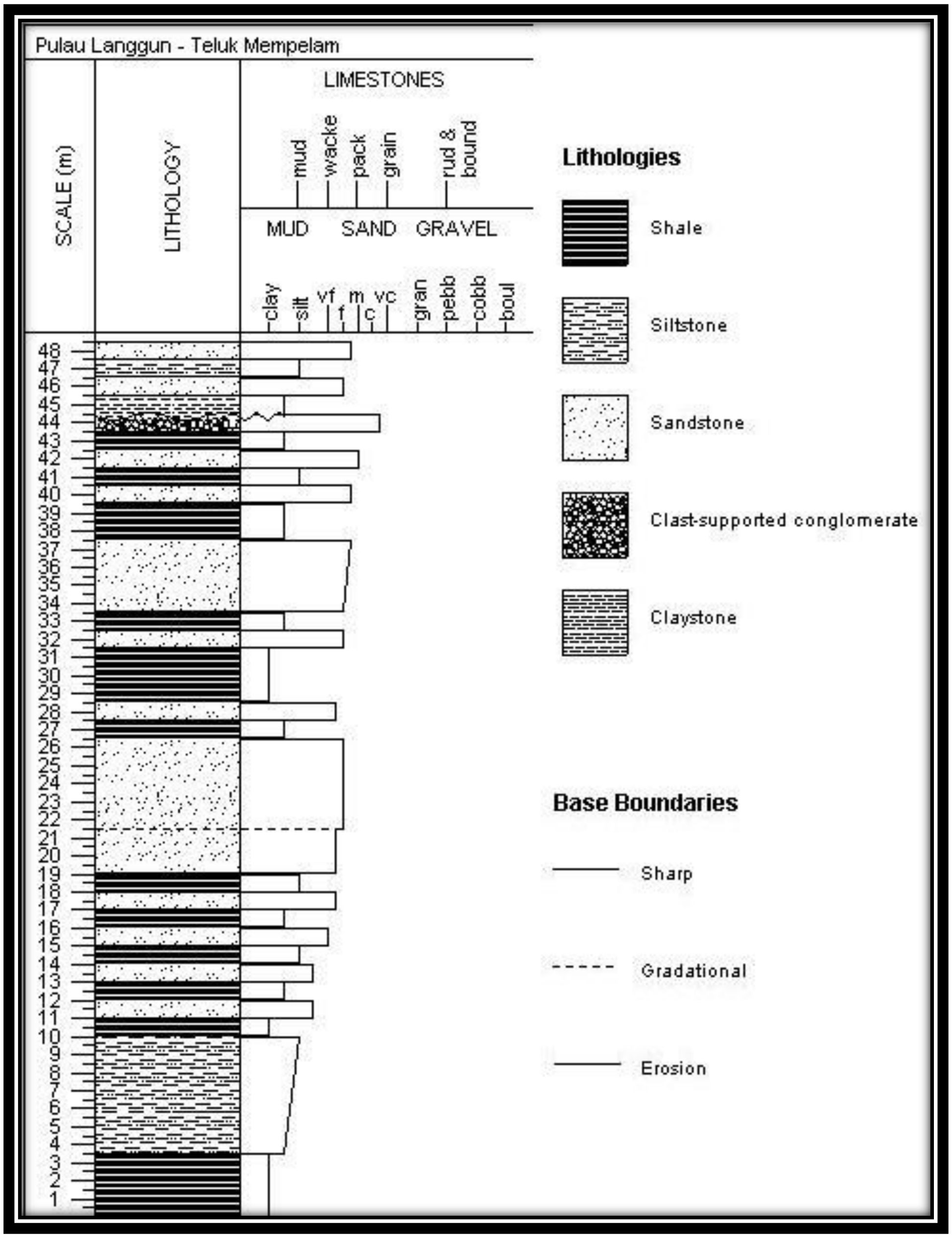


Figure 35: Sedimentary logging of the northern part of Teluk Mempelam. From 0 m – 44.5 m is the Timah Tasoh Formation, while from 44.5 m – 48.5 m is the Langgun Red Beds.

The sedimentary log shows the variation of facies as we walk further north of Teluk Mempelam. The sequence of the grains can be seen to be coarsening upwards, which corresponds to its depositional environment i.e. from deep to shallow marine. From the log, it can be seen that the outcrops at the study area is sandstone interbedded with shale. Towards the southern part, the units can be seen to have finer grains, almost silty.

## 4.5. Mineralogy

### 4.5.1. Thin Section

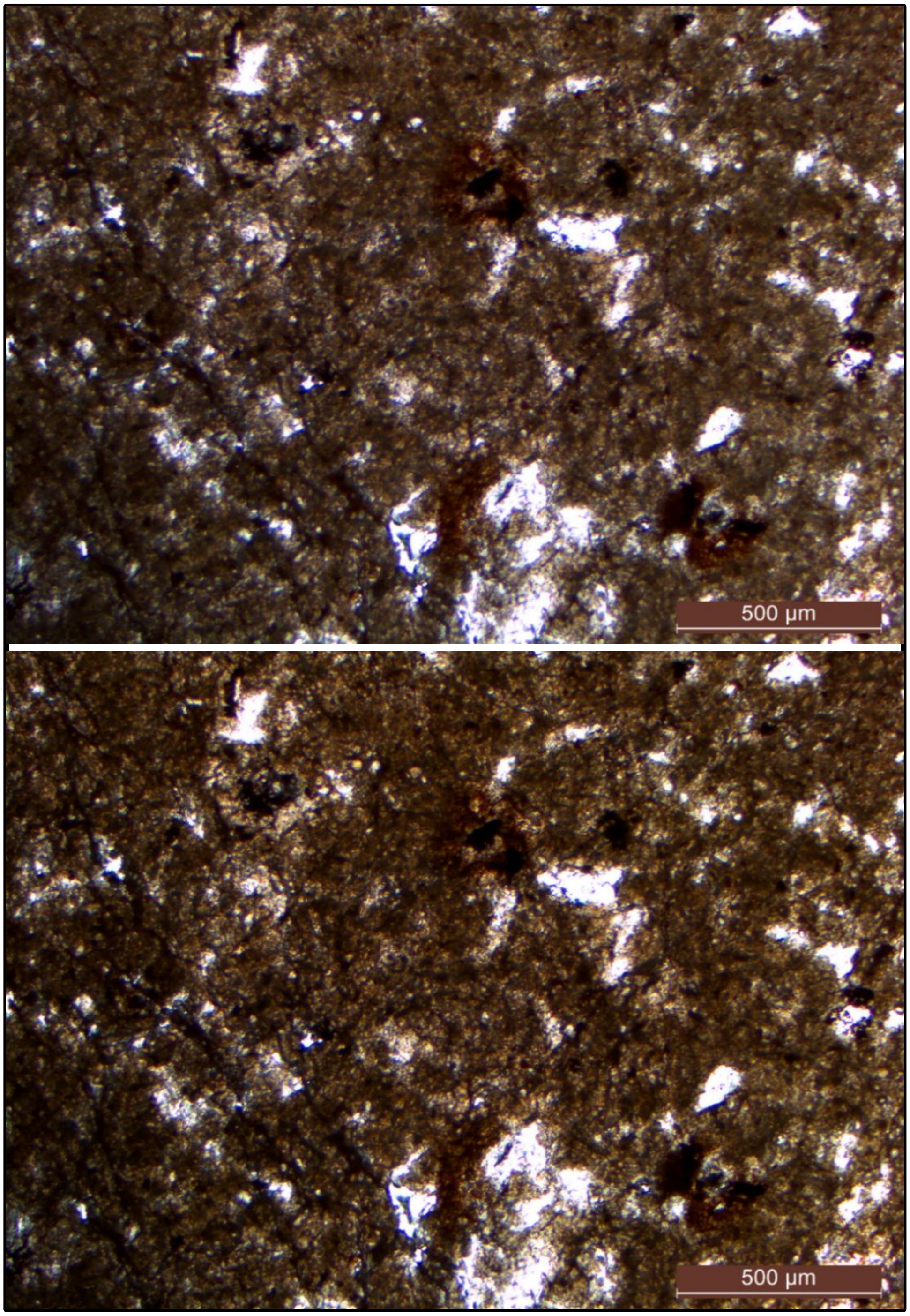


Figure 36: Sample of thin section from Langgun Red Beds (TOP: Plane polarised light, or PPL; BOTTOM: Cross polarised light, or XPL).

The grains are seen to be silty in nature and mostly made up of quartz, highlighted by the extinction and the lack of birefringence.

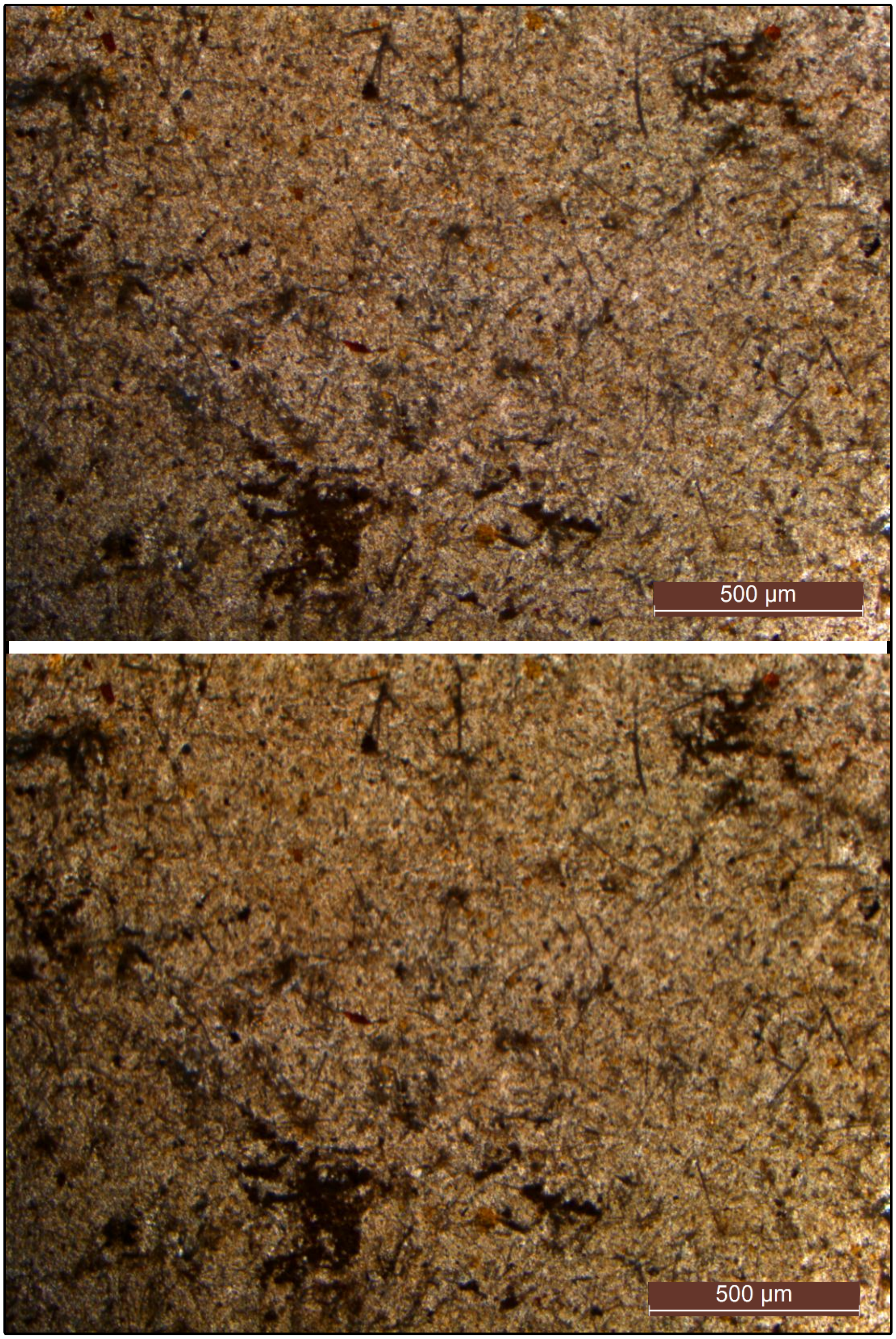


Figure 37: Sample of thin section from red shale from Timah Tasoh Formation (TOP: PPL; BOTTOM: XPL).

Quartz grains are scattered, characterised by the high extinction and low birefringence, which gives off the colour brown in XPL. There is also iron oxide characterised by the dark brown needle- like structures.

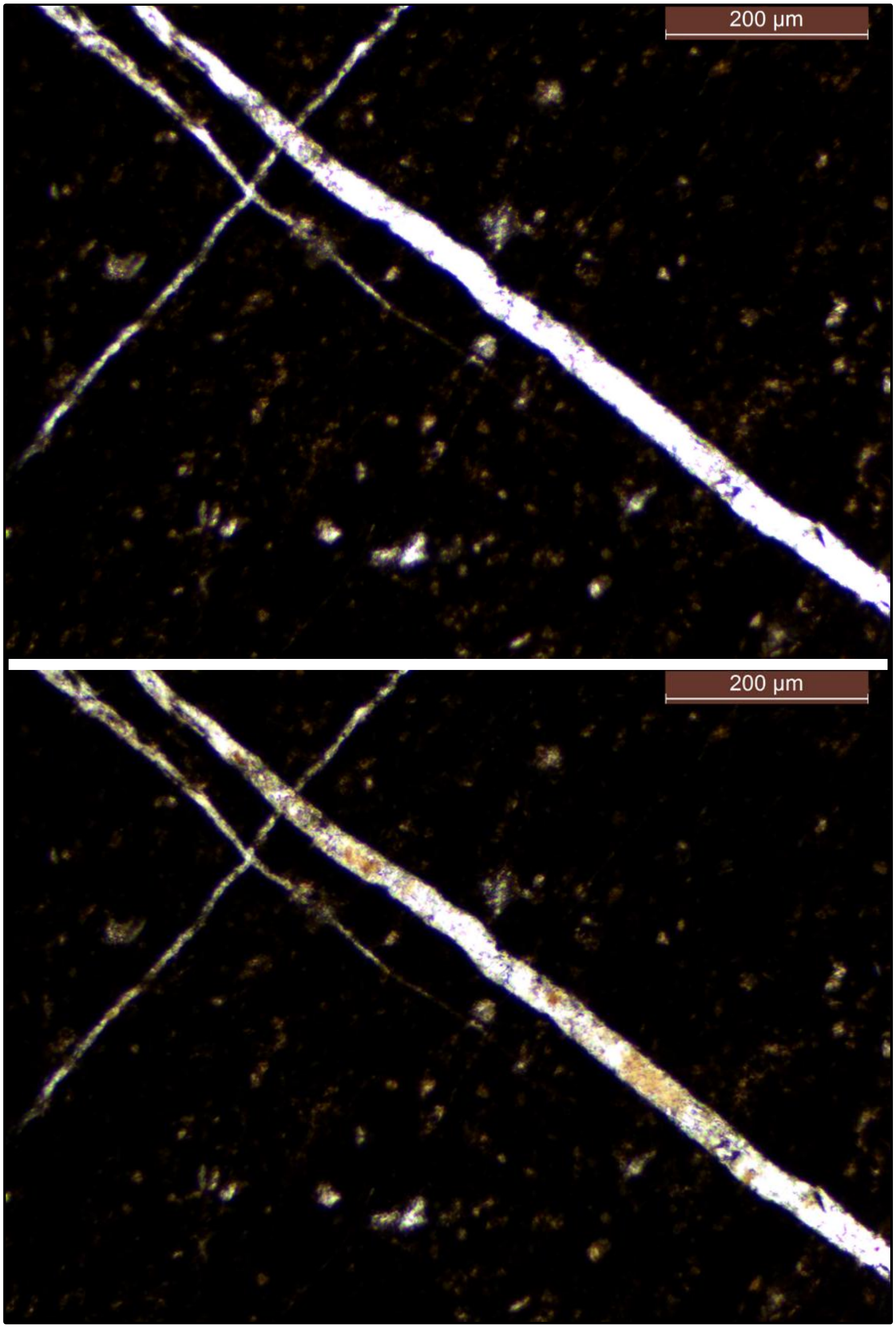

Figure 38: Sample of thin section from grey shale from Timah Tasoh Formation at 130$^{o}$ (TOP: PPL; BOTTOM: XPL).

Dark matrix with scattered quartz grains can be seen. There is also a quartz infill, noted by the brown extinction.

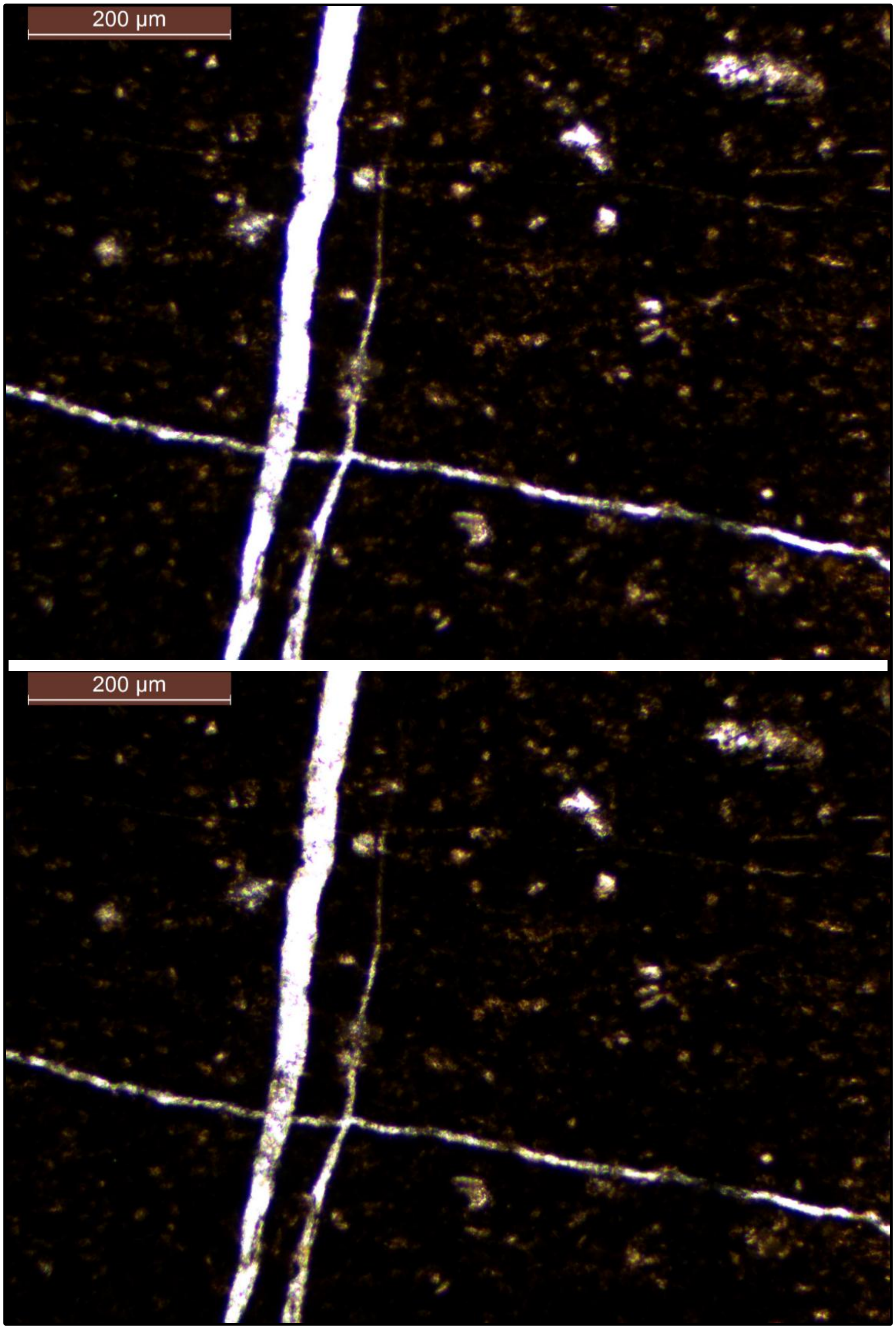


Figure 39: Sample of thin section from grey shale from Timah Tasoh Formation rotated to 250° (TOP: PPL; BOTTOM: XPL).

It can be seen when rotated to this angle; the extinction is gone, further confirming that the infill is by quartz.

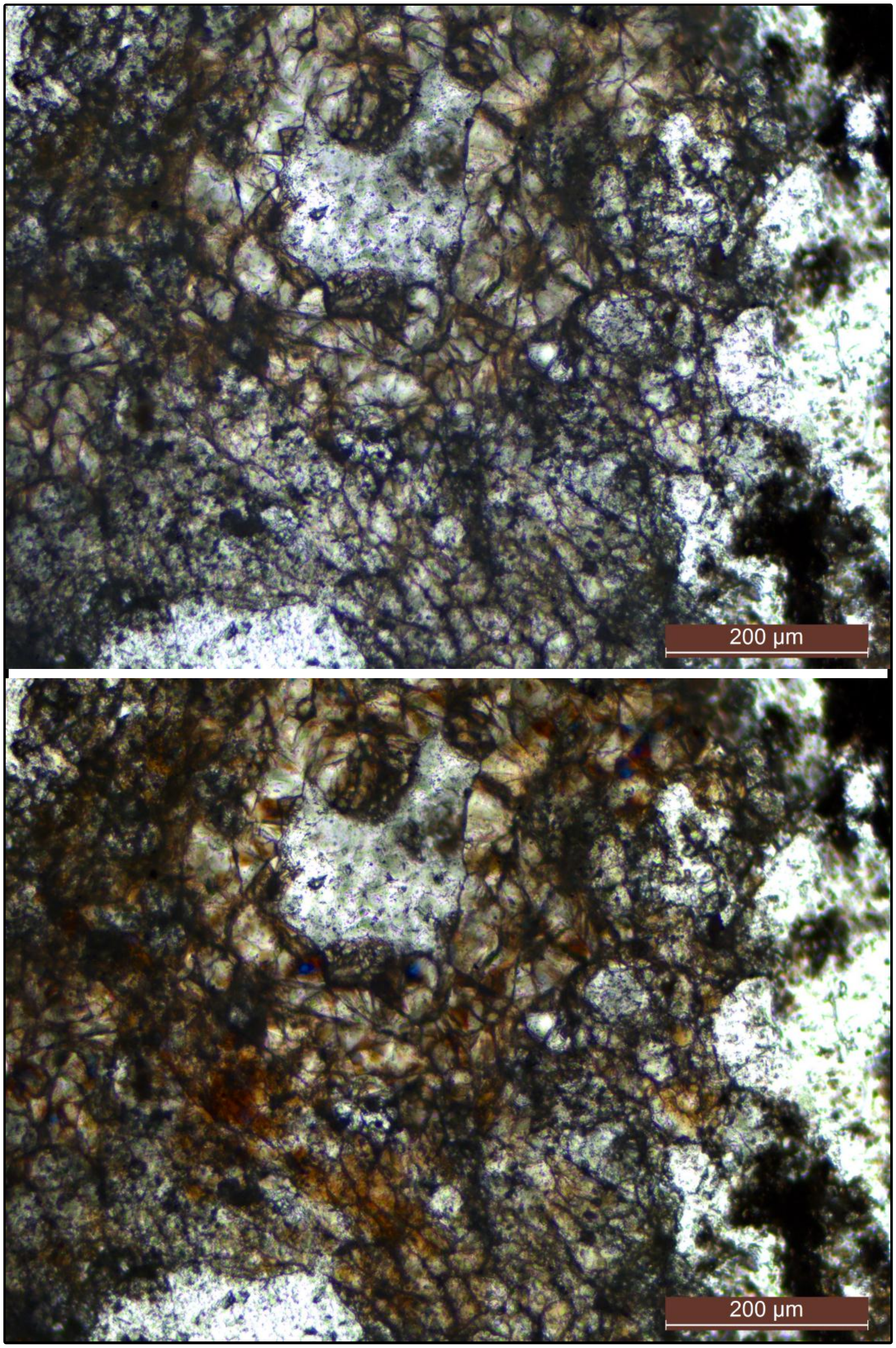

Figure 40: Sample of thin section from black shale from Timah Tasoh Formation (TOP: PPL; BOTTOM: XPL).

Quartz grains can be seen, characterised by the high extinction and low birefringence, which gives off the colour brown in XPL.

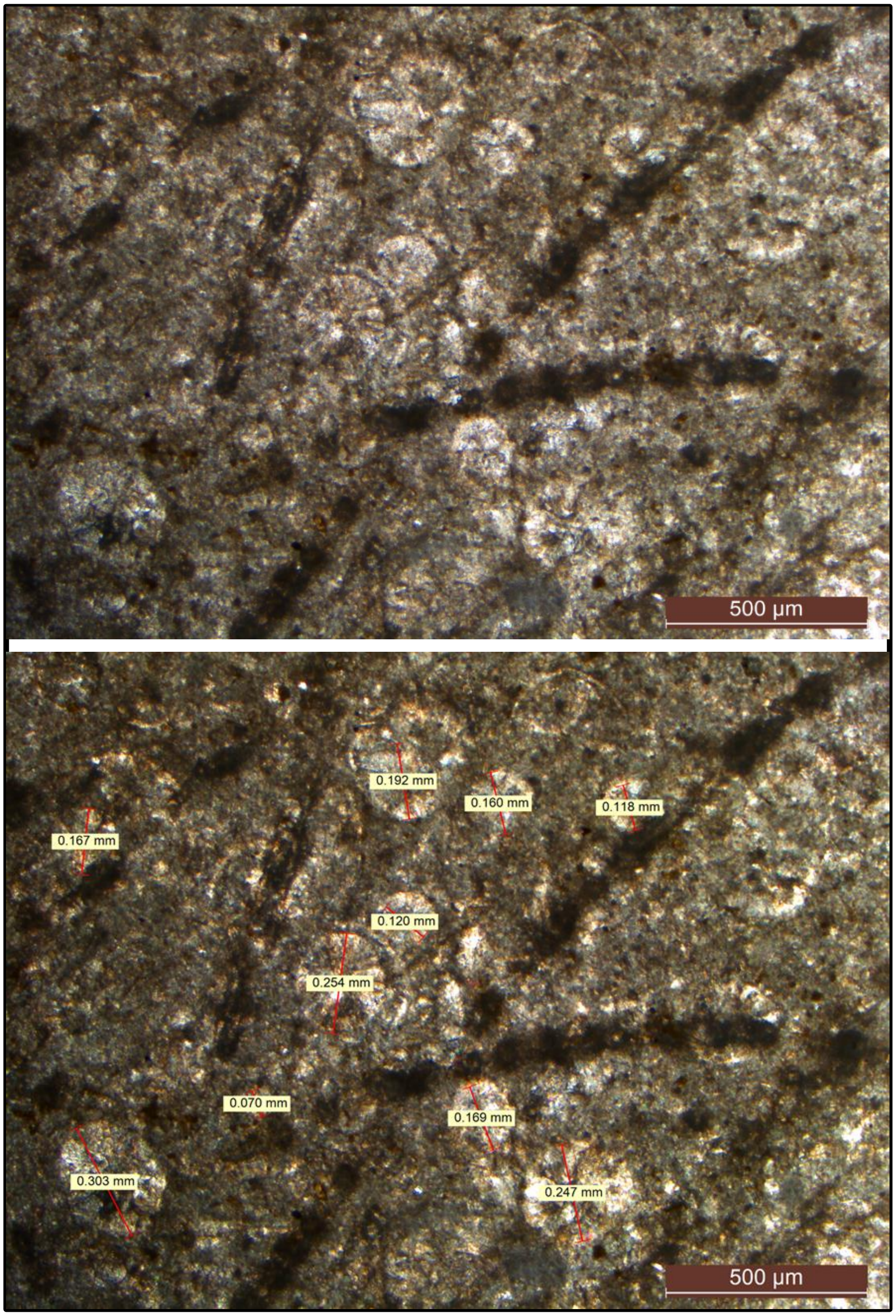

Figure 41: Sample of thin section from Mempelam Limestone (TOP: PPL; BOTTOM: XPL).

Calcitic matrix is abundant, thus it is matrix supported. However, it is good to note that there are also a lot of circular grains, which is probably ooids or calcite-replaced fossil fragments.

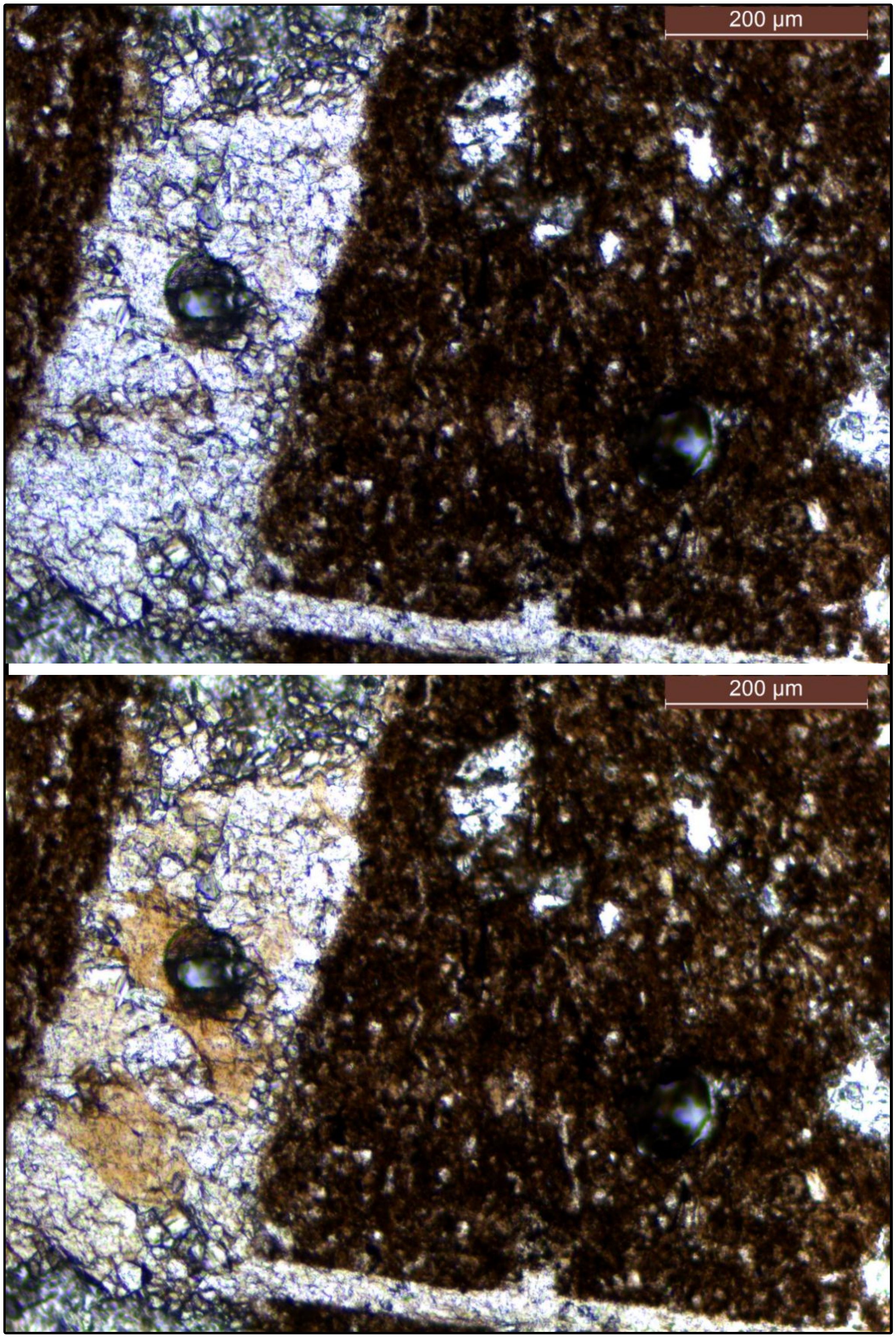

Figure 42: Sample of thin section from Tanjong Dendang Formation at $0^o$ (TOP: PPL; BOTTOM: XPL).

Dark matrix with scattered quartz grains can be seen. There is also a quartz infill, noted by the brown extinction.

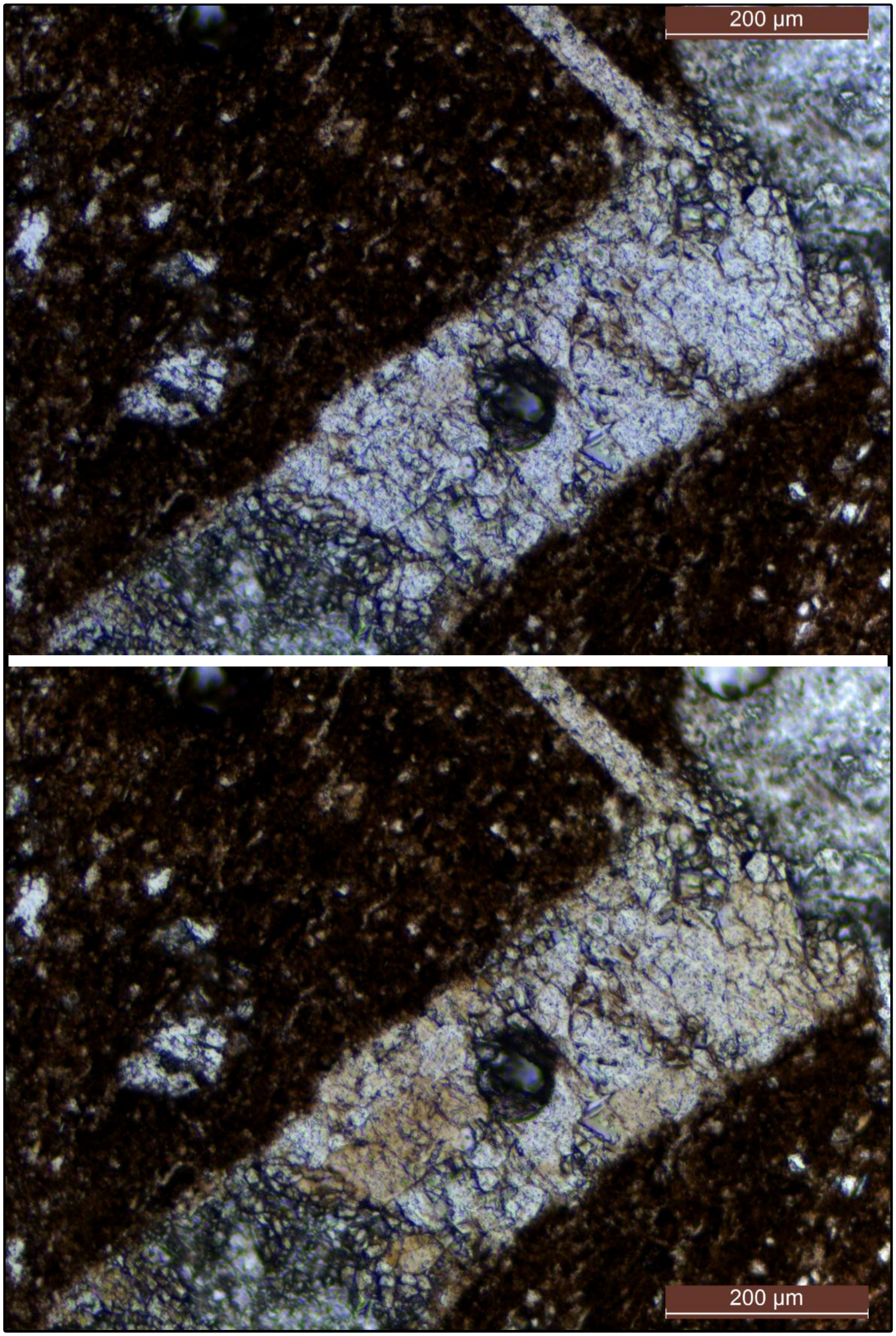


Figure 43: Sample of thin section from Tanjong Dendang Formation rotated to 145$^{o}$ (TOP: PPL; BOTTOM: XPL).

It can be seen when rotated to this angle; the extinction is gone, further confirming that the infill is by quartz.

### 4.5.2. X–Ray Fluorescence

X-Ray fluorescence focuses on the element content of the sample. It was decided that the most prominent elements are noted in the results. The rest are trace elements inside the samples.

Table 3: Results of X–Ray Fluorescence.

| CONCENTRATION | SAMPLE 1 | SAMPLE 2 | SAMPLE 3 | SAMPLE 4 | SAMPLE 5 | SAMPLE 6 |
|---|---|---|---|---|---|---|
| Silicon (%) | 63.7 | 62.7 | 75.4 | 57.1 | 1.86 | 80.9 |
| Potassium (%) | 9.62 | 8.95 | 5.48 | 11.2 | 0.744 | 6.79 |
| Iron (%) | 10.7 | 13.6 | 8.96 | 8.75 | 1.08 | 3.87 |
| Aluminium (%) | 9.67 | 8.82 | 4.04 | 6.95 | 0.539 | 2.85 |
| Chlorine (%) | 0.754 | 0.823 | 0.512 | 2.96 | 0.0974 | 0.757 |
| Barium (%) | 0.638 | Nil | 0.739 | 2.20 | Nil | Nil |
| Phosphorus (%) | 1.50 | 1.61 | 1.85 | 3.65 | 0.278 | 1.62 |
| Calcium (%) | 0.885 | 0.811 | 1.05 | 1.70 | 94.6 | 1.01 |
| Magnesium (%) | 0.355 | 0.346 | 0.322 | 0.551 | 0.313 | 0.159 |
| Titanium (%) | 1.35 | 1.35 | 0.698 | 1.68 | 0.153 | 0.624 |

**Note: Sample 1 is taken from Langgun Red Beds, Sample 2 is taken from red shale of Timah Tasoh Formation, Sample 3 is taken from grey shale of Timah Tasoh Formation, Sample 4 is taken from black shale of Timah Tasoh Formation, Sample 5 is taken from Mempelam Limestone, and Sample 6 is taken from Tanjong Dendang Formation.**

These results further confirm the interpretations of the thin sections. The major element in the clastics samples is silicon, which is the main element for quartz. While, the iron is probably contributed from the infill of the conjugate joints as seen in Chapter 4.1.

Whereas, the major element in the carbonate sample is calcium, which is the main element for calcite.

## 4.6. Source Rock Potential

### 4.6.1. Total Carbon Analysis (TCA)

TCA is the first chemical analysis to be carried out to assess the potential for petroleum source rock. The classification for TCA can be seen in Figure 44.

| Total Organic Content, Weight % | Kerogen Quality |
|---|---|
| < 0.5 | Very poor |
| 0.5 to 1 | Poor |
| 1 to 2 | Fair |
| 2 to 4 | Good |
| 4 to 12 | Very good |
| > 12 | Excellent |

Figure 44: Organic content of source rock.

The results for the samples from Teluk Mempelam can be observed in Table 4.

Table 4: Result of the Total Carbon analysis

| CONCENTRATION | SAMPLE 1 | SAMPLE 2 | SAMPLE 3 | SAMPLE 4 | SAMPLE 5 | SAMPLE 6 |
|---|---|---|---|---|---|---|
| Total Organic Carbon (wt%) | 0.177 | 0.263 | 0.952 | 9.91 | 2.12 | 1.32 |
| Total Inorganic Carbon (wt%) | 0.088 | 0.05 | 0.198 | 0 | 8.88 | 0.21 |
| Total Carbon (wt%) | 0.265 | 0.313 | 1.15 | 9.91 | 11 | 1.53 |

**Note: Sample 1 is taken from Langgun Red Beds, Sample 2 is taken from red shale of Timah Tasoh Formation, Sample 3 is taken from grey shale of Timah Tasoh Formation, Sample 4 is taken from black shale of Timah Tasoh Formation, Sample 5 is taken from Mempelam Limestone, and Sample 6 is taken from Tanjong Dendang Formation.**

Sample 1 and 2 has a very poor total organic content, while sample 3 has a poor total organic content with quite significant inorganic carbon content. However, sample 4 possesses a very good total organic carbon content with no inorganic carbon content at all. For the only carbonate in the samples, sample 5 has a higher degree of inorganic carbon because of its carbonate properties. However, its organic carbon content is still good. Sample 6 contains a fair amount of organic carbon.

## 4.7. Graptolite Morphology

Previous works on graptolites of Pulau Langgun were obtained and studied to compare with the ones found for the research.


Figure 45: Graptolite fossil found by Jones (1976).

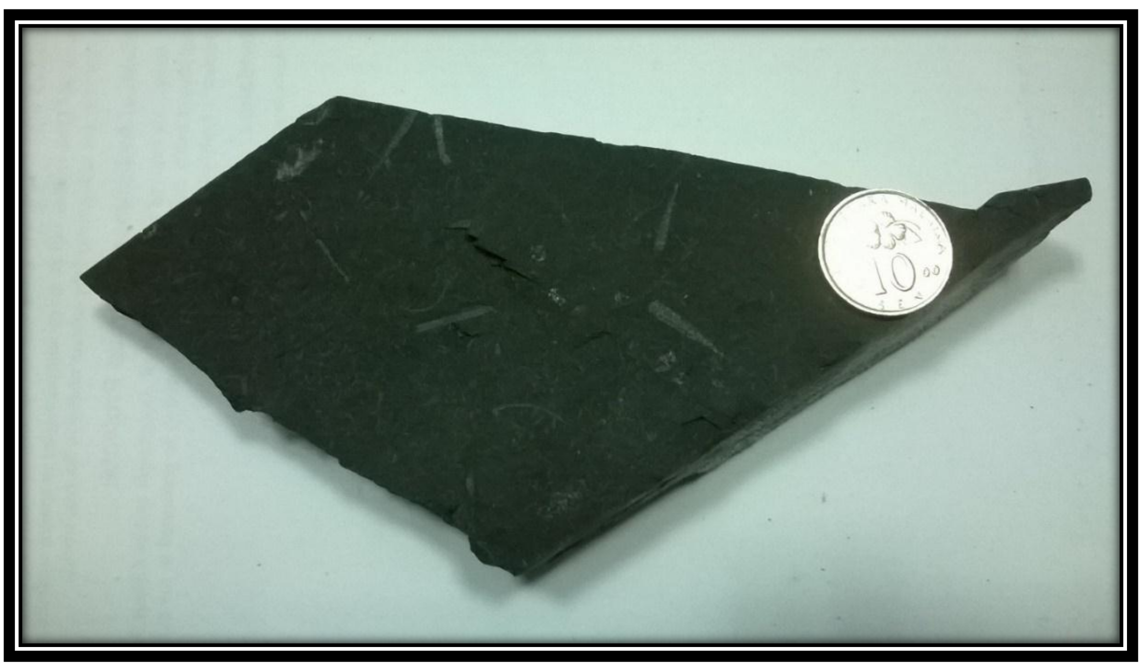


Figure 46: Graptolite fossils found by Jones (1976).

Figure 47: Graptolite fossils found by Jones (1976).

The samples are observed and sketched for identification of the graptolite respective genera.

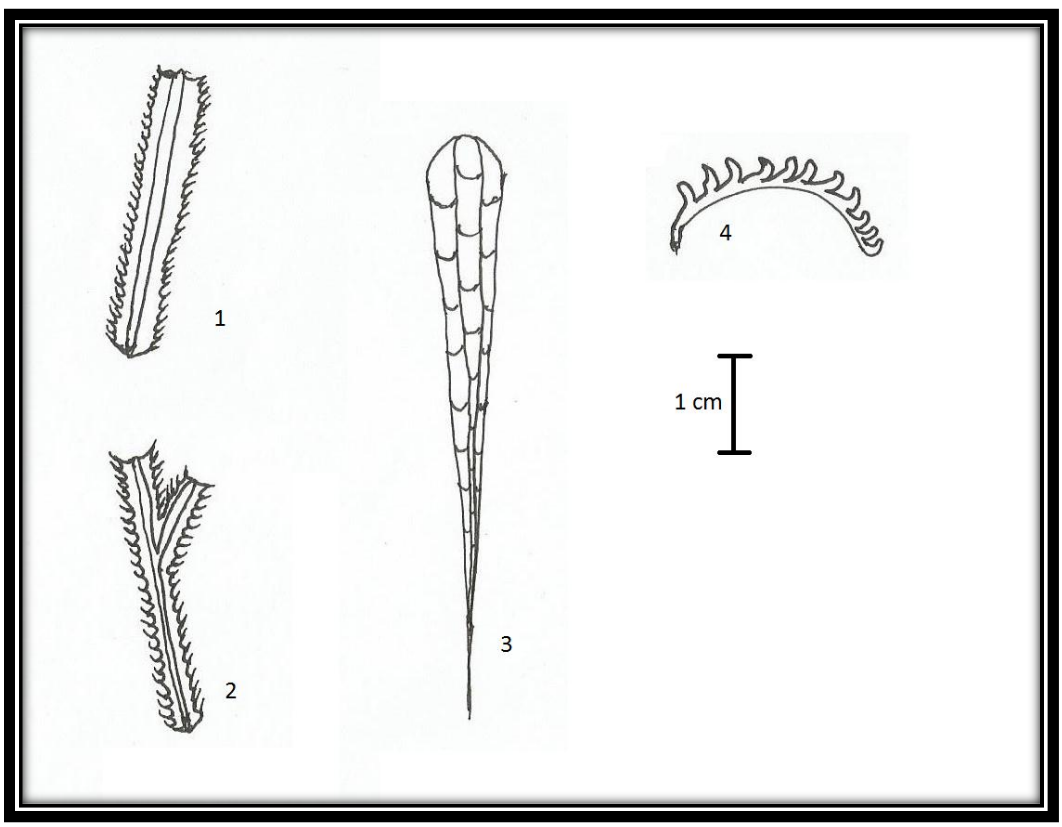


Figure 48: Sketches of the Graptolites found in the previous works on graptolites in study area. 1 & 2: Glyptograptus sp.; 3: Dimorphograptus sp.; 4: Pristiograptus sp.

The classifications of such genera are listed below:

*Glyptograptus sp.*

| | |
|---|---|
| Kingdom | : Animalia |
| Phylum | : Hemichordata |
| Class | : Graptolithina |
| Order | : Graptoloidea |
| Family | : Glyptograptidae |
| Genus | : Glyptograptus |

*Dimorphograptus sp.*

| | |
|---|---|
| Kingdom | : Animalia |
| Phylum | : Hemichordata |
| Class | : Graptolithina |
| Order | : Graptoloidea |
| Family | : Dimorphograptidae |
| Genus | : Dimorphograptus |

*Pristiograptus sp.*

| | |
|---|---|
| Kingdom | : Animalia |
| Phylum | : Hemichordata |
| Class | : Graptolithina |
| Order | : Graptoloidea |
| Family | : Monograptidae |
| Genus | : Pristiograptus |

A sample with graptolite fossils are found on the study area, particularly on the parts of the island exposed with the Tanjong Dendang Formation.

Figure 49: The graptolite fossils found for this research.

The samples are observed and sketched for identification of the graptolite respective genera. The sample will be sent to experts to further identify the species present.

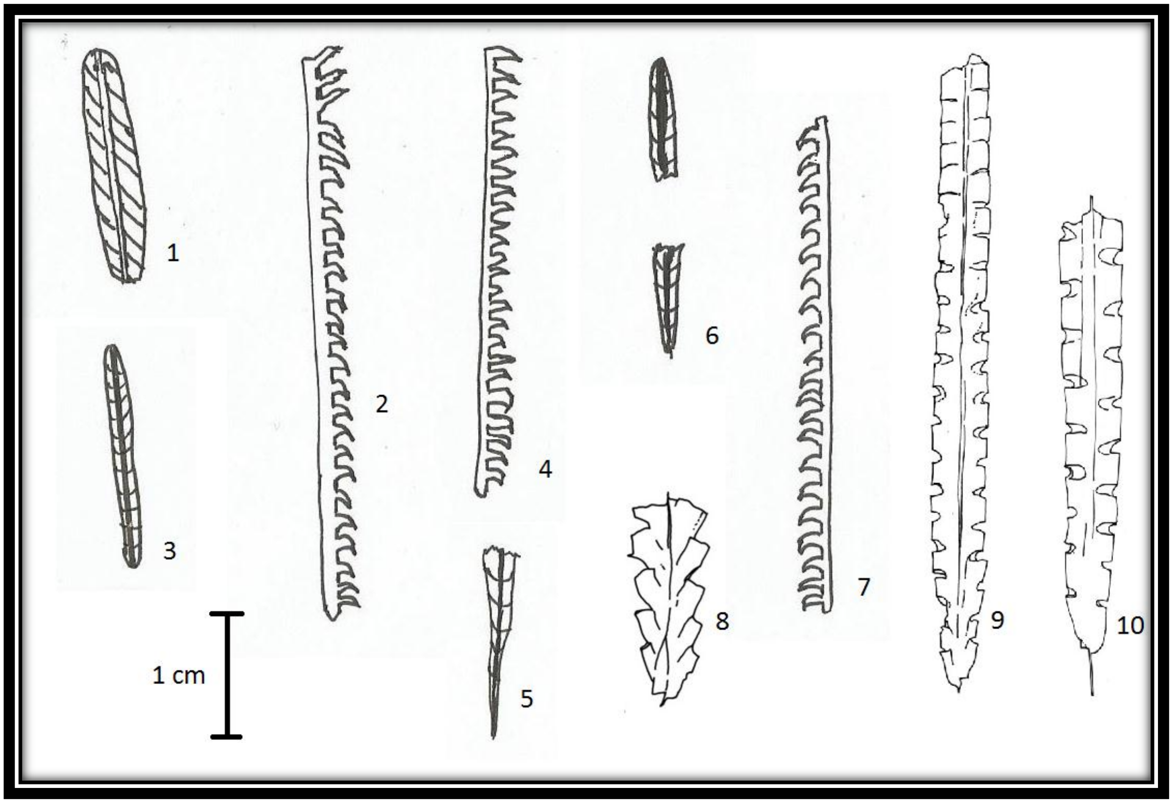

Figure 50: The sketches of the fossils observed from the sample found on study area. 1, 3, 5, 6, 8, 9 & 10: Dimorphograptus sp.; 2, 4 & 7: Glyptograptus sp.

It is known that *Dimorphograptus* sp. exists in the lower Silurian, while *Glyptograptus* sp. exists in the Ordovician-Silurian. The sample taken from the study area for observation is pinpointed to be from the lower Silurian based on the fossils identified from the sketches. The depositional environment is also determined to be low-energy deep marine environments due to the nature of the graptolites.

The sample will be sent to experts on graptolites to further identify the species of the graptolites present.

# CHAPTER 5

# CONCLUSION AND RECOMMENDATION

Based on the literature review and pre-analysis that had been conducted during the fieldwork, Teluk Mempelam is indeed a unique geologic feature in that you can walk through the whole Ordovician-Carboniferous geologic record, from older rocks in the south to younger rocks in the north. Four types of lithology are found to be deposited in that area, namely dark-colored limestone, siltstone with sandstone lenses, mudstone and shale interbedded with carbonaceous mudstone.

Pulau Langgun is indeed rich in its fossil occurrences as mentioned by several previous work specifically Teluk Mempelam. The fossils emphasised is the graptolites found on the study area. The occurring graptolites found on the specimen used for this research are *Glyptograptus* sp., *Dimorphograptus* sp., & *Pristiograptus* sp. This leads to the assumption that the date of the outcrop is relatively lower Silurian. These fossil occurrences indicates the depositional environment of low-energy, deep marine environment. While, the source rock potential for the outcrops of Teluk Mempelam are poor to very good.

It is recommended for future works to possibly use the graptolites fossil to integrate with a more detailed study of the palaeogeography of Pulau Langgun. As one of the recommendations, future researchers could focus their study more in-depth about the source rock potential of Paleozoic rocks of Malaysia with Pulau Langgun as analogy. Since graptolites can be used as an indicator for the maturity of the source rock and such works have also been used in a number of studies, one of which is Goodarzi & Norford (1987), Malaysian graptolites should be studied in such a way for such applications would prove to be useful, especially in the oil & gas industry.

# REFERENCES

Benton, M. J., & Harper, D. A. (2009). *Introduction to Paleobiology and the Fossil Record.* New York, United States of America: Wiley-Blackwell.

Cocks, L., Fortey, R. A., & Lee, C. P. (2005). A review of Lower and Middle Palaeozoic biostratigraphy in west peninsular Malaysia and southern Thailand in its context within the Sibumasu Terrane. *Journal of Asian Earth Sciences 24*, 703–717.

Gobbett, D. J., & Hutchison, C. S. (1973). *Geology of the Malay Peninsula.* New York, United States of America: Wiley-Interscience.

Goodarzi, F., & Norford, B. S. (1987). Optical properties of graptolite epiderm—a review. *Bulletin of Geology Society Denmark, 35*, 141-147.

Jones, C. R. (1976). *The geology and mineral resources of Perlis, North Kedah, and the Langkawi Islands.* Kuala Lumpur: Geological Survey of Malaysia.

Kobayashi, T., & Hamada, T. (1978). Upper Ordovician trilobites from the Langkawi Islands, Malaysia. *Geology and Palaeontology of Southeast Asia 19*, 1–27.

Lee, C. P. (2009). Palaeozoic Stratigraphy. In C. R. Hutchison, & D. N. Tan, *Geology of Peninsular Malaysia* (pp. 55-86). Kuala Lumpur: University of Malaya and Geological Society of Malaysia.

Meor Hakif Amir Hassan. (2013). Post-Conference Field Excursion to Northwest Peninsular Malaysia. *Third International Conference on Palaeontology of South East Asia: ICPSEA 3* (pp. 23-25). Kuala Lumpur: Universiti Malaya. Retrieved February 25, 2014, from http://umexpert.um.edu.my/file/publication/00006513_97630.pdf

Wicander, R., & Monroe, J. S. (2009). Essentials of Physical Geology: Brooks/Cole, Cengage Learning.

Wyatt, D., Stait, B., & Burrett, C. (1983). The Ordovician system in southern Thailand and northern. In P. Nutalaya, *Stratigraphic correlation of Thailand and Malaysia* (pp. 77-95). Bangkok: Geological Societies of Thailand and Malaysia.

# APPENDICES

# APPENDIX A: X-Ray Fluorescence results

Eval2 - [Quant] - [JOHAN BS]

File View Quanti Window Tools Help

Active sample: JOHAN BS

Intensity Scale: 3.801 Compton ratio: 8.78 %

| Concentration | Formula | Z | Status | Line 1 | Stat. error | Net int. | Calc. co... | LLD | Analyzed layer |
|---|---|---|---|---|---|---|---|---|---|
| 57.1 % | Si | 14 | XRF 1 | Si KA1-HR-Tr | 0.822 % | 189.7 | 57.1 | 233.4 ... | 6.6 um |
| 11.2 % | K | 19 | XRF 1 | K KA1-HR-Tr | 1.56 % | 52.85 | 11.2 | | 9.5 um |
| 8.75 % | Fe | 26 | XRF 1 | Fe KA1-HR-Tr | 0.784 % | 211.2 | 8.75 | 111.3 ... | 40 um |
| 6.95 % | Al | 13 | XRF 1 | Al KA1-HR-Tr | 2.65 % | 18.18 | 6.95 | | 5.6 um |
| 3.65 % | P | 15 | XRF 1 | P KA1-HR-Tr | 3.60 % | 10.23 | 3.65 | 367.8 ... | 2.93 um |
| 2.96 % | Cl | 17 | XRF 1 | Cl KA1-HR-Tr | 3.84 % | 9.993 | 2.96 | 547.6 ... | 5.3 um |
| 2.20 % | Ba | 56 | XRF 1 | Ba LA1-HR-Tr | 5.74 % | 4.250 | 2.20 | 0.142 % | 16.5 um |
| 1.75 % | S | 16 | XRF 1 | S KA1-HR-Tr | 3.89 % | 9.364 | 1.75 | 323.1 ... | 3.8 um |
| 1.70 % | Ca | 20 | XRF 1 | Ca KA1-HR-Tr | 4.09 % | 8.007 | 1.70 | 582.1 ... | 10.3 um |
| 1.68 % | Ti | 22 | XRF 1 | Ti KA1-HR-Tr | 3.60 % | 10.27 | 1.68 | 305.0 ... | 17.0 um |
| 0.551 % | Mg | 12 | XRF 1 | Mg KA1-HR-Tr | 11.3 % | 1.294 | 0.55 | 320.3 ... | 3.7 um |
| 0.345 % | Sr | 38 | XRF 1 | Sr KA1-HR-Tr | 1.78 % | 59.23 | 0.345 | 46.3 PPM | 288 um |
| 0.308 % | V | 23 | XRF 1 | V KA1-HR-Tr | 6.88 % | 3.162 | 0.31 | 498.6 ... | 21.9 um |
| 0.217 % | Rb | 37 | XRF 2 | Rb KA1-HR-Tr | 7.73 % | 8.302 | 0.044 | 81.1 PPM | 245 um |
| 0.140 % | Cu | 29 | XRF 1 | Cu KA1-HR-Tr | 6.18 % | 6.334 | 0.14 | 79.2 PPM | 59 um |
| 0.119 % | Ni | 28 | XRF 1 | Ni KA1-HR-Tr | 7.90 % | 4.223 | 0.12 | 89.4 PPM | 48 um |
| 0.0448 % | Br | 35 | XRF 1 | Br KA1-HR-Tr | 12.5 % | 4.297 | 0.045 | 79.6 PPM | 176 um |
| 0.0448 % | Mo | 42 | XRF 1 | Mo KA1-HR-Tr | 8.41 % | 9.734 | 0.045 | 45.4 PPM | 0.51 mm |
| 0.0380 % | Se | 34 | XRF 1 | Se KA1-HR-Tr | 20.1 % | 2.374 | 0.038 | 94.6 PPM | 148 um |
| 0.0323 % | As | 33 | XRF 1 | As KA1-HR-Tr | 15.1 % | 3.019 | 0.032 | 58.7 PPM | 124 um |
| 86.053 PPM | Cr | 24 | XRF 1 | Cr KA1-HR-Tr | 13.3 % | 1.586 | 0.009 | 580.5 ... | 26.0 um |

Eval2 - [Quant] - [JOHAN GS]

File View Quanti Window Tools Help

Active sample: JOHAN GS

Intensity Scale: 4.032 Compton ratio: 10.1 %

| Concentration | Formula | Z | Status | Line 1 | Stat. error | Net int. | Calc. co... | LLD | Analyzed layer |
|---|---|---|---|---|---|---|---|---|---|
| 75.4 % | Si | 14 | XRF 1 | Si KA1-HR-Tr | 0.704 % | 258.7 | 75.4 | 209.6 ... | 8.0 um |
| 8.96 % | Fe | 26 | XRF 1 | Fe KA1-HR-Tr | 0.742 % | 235.9 | 8.96 | 95.4 PPM | 45 um |
| 5.48 % | K | 19 | XRF 1 | K KA1-HR-Tr | 2.30 % | 24.25 | 5.48 | | 8.8 um |
| 4.04 % | Al | 13 | XRF 1 | Al KA1-HR-Tr | 3.41 % | 11.01 | 4.04 | | 6.3 um |
| 1.85 % | P | 15 | XRF 1 | P KA1-HR-Tr | 5.60 % | 4.431 | 1.85 | 335.9 ... | 2.47 um |
| 1.05 % | Ca | 20 | XRF 1 | Ca KA1-HR-Tr | 5.19 % | 5.068 | 1.05 | 412.7 ... | 10.6 um |
| 0.739 % | Ba | 56 | XRF 1 | Ba LA1-HR-Tr | 10.5 % | 1.472 | 0.74 | 995.2 ... | 17.2 um |
| 0.698 % | Ti | 22 | XRF 1 | Ti KA1-HR-Tr | 14.0 % | 4.461 | 0.70 | 216.7 ... | 17.7 um |
| 0.512 % | Cl | 17 | XRF 1 | Cl KA1-HR-Tr | 12.8 % | 1.533 | 0.51 | 515.6 ... | 4.6 um |
| 0.394 % | S | 16 | XRF 1 | S KA1-HR-Tr | 10.3 % | 1.826 | 0.39 | 280.2 ... | 3.3 um |
| 0.322 % | Mg | 12 | XRF 1 | Mg KA1-HR-Tr | 14.5 % | 0.7997 | 0.32 | 224.3 ... | 4.1 um |
| 0.0614 % | Cr | 24 | XRF 1 | Cr KA1-HR-Tr | 22.7 % | 0.7752 | 0.061 | 138.5 ... | 28.5 um |
| 0.0383 % | Rb | 37 | XRF 1 | Rb KA1-HR-Tr | 9.53 % | 6.472 | 0.038 | 45.0 PPM | 272 um |
| 0.0361 % | Cu | 29 | XRF 1 | Cu KA1-HR-Tr | 18.1 % | 1.734 | 0.036 | 69.7 PPM | 64 um |
| 0.0358 % | Ni | 28 | XRF 1 | Ni KA1-HR-Tr | 20.7 % | 1.352 | 0.036 | 79.1 PPM | 52 um |
| 0.0241 % | Sr | 38 | XRF 1 | Sr KA1-HR-Tr | 13.9 % | 4.539 | 0.024 | 37.8 PPM | 0.32 mm |
| 0.0221 % | As | 33 | XRF 1 | As KA1-HR-Tr | 19.7 % | 2.205 | 0.022 | 48.7 PPM | 137 um |
| 0.0220 % | Zr | 40 | XRF 1 | Zr KA1-HR-Tr | 6.43 % | 11.76 | 0.022 | 74.7 PPM | 0.44 mm |
| 0.0174 % | Nb | 41 | XRF 1 | Nb KA1-HR-Tr | 18.4 % | 3.945 | 0.017 | 39.1 PPM | 0.51 mm |

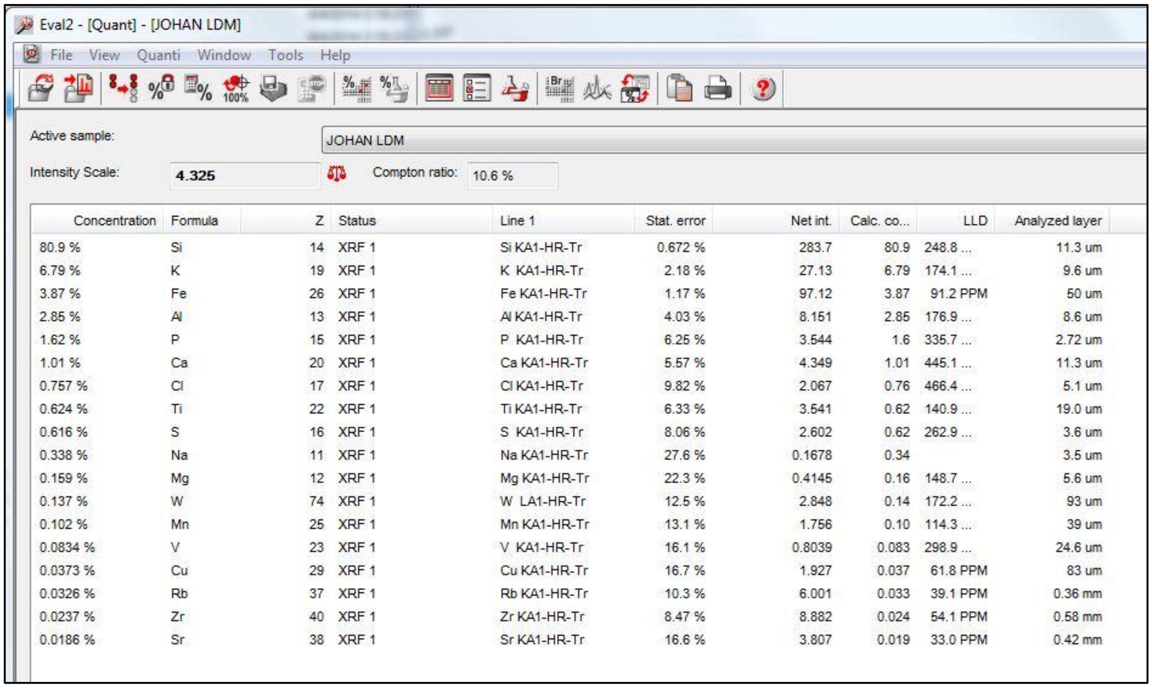

Eval2 - [Quant] - [JOHAN LDM]

File View Quanti Window Tools Help

Active sample: JOHAN LDM

Intensity Scale: 4.325 Compton ratio: 10.6 %

| Concentration | Formula | Z | Status | Line 1 | Stat. error | Net int. | Calc. co... | LLD | Analyzed layer |
|---|---|---|---|---|---|---|---|---|---|
| 80.9 % | Si | 14 | XRF 1 | Si KA1-HR-Tr | 0.672 % | 283.7 | 80.9 | 248.8 ... | 11.3 um |
| 6.79 % | K | 19 | XRF 1 | K KA1-HR-Tr | 2.18 % | 27.13 | 6.79 | 174.1 ... | 9.6 um |
| 3.87 % | Fe | 26 | XRF 1 | Fe KA1-HR-Tr | 1.17 % | 97.12 | 3.87 | 91.2 PPM | 50 um |
| 2.85 % | Al | 13 | XRF 1 | Al KA1-HR-Tr | 4.03 % | 8.151 | 2.85 | 176.9 ... | 8.6 um |
| 1.62 % | P | 15 | XRF 1 | P KA1-HR-Tr | 6.25 % | 3.544 | 1.6 | 335.7 ... | 2.72 um |
| 1.01 % | Ca | 20 | XRF 1 | Ca KA1-HR-Tr | 5.57 % | 4.349 | 1.01 | 445.1 ... | 11.3 um |
| 0.757 % | Cl | 17 | XRF 1 | Cl KA1-HR-Tr | 9.82 % | 2.067 | 0.76 | 466.4 ... | 5.1 um |
| 0.624 % | Ti | 22 | XRF 1 | Ti KA1-HR-Tr | 6.33 % | 3.541 | 0.62 | 140.9 ... | 19.0 um |
| 0.616 % | S | 16 | XRF 1 | S KA1-HR-Tr | 8.06 % | 2.602 | 0.62 | 262.9 ... | 3.6 um |
| 0.338 % | Na | 11 | XRF 1 | Na KA1-HR-Tr | 27.6 % | 0.1678 | 0.34 | | 3.5 um |
| 0.159 % | Mg | 12 | XRF 1 | Mg KA1-HR-Tr | 22.3 % | 0.4145 | 0.16 | 148.7 ... | 5.6 um |
| 0.137 % | W | 74 | XRF 1 | W LA1-HR-Tr | 12.5 % | 2.848 | 0.14 | 172.2 ... | 93 um |
| 0.102 % | Mn | 25 | XRF 1 | Mn KA1-HR-Tr | 13.1 % | 1.756 | 0.10 | 114.3 ... | 39 um |
| 0.0834 % | V | 23 | XRF 1 | V KA1-HR-Tr | 16.1 % | 0.8039 | 0.083 | 298.9 ... | 24.6 um |
| 0.0373 % | Cu | 29 | XRF 1 | Cu KA1-HR-Tr | 16.7 % | 1.927 | 0.037 | 61.8 PPM | 83 um |
| 0.0326 % | Rb | 37 | XRF 1 | Rb KA1-HR-Tr | 10.3 % | 6.001 | 0.033 | 39.1 PPM | 0.36 mm |
| 0.0237 % | Zr | 40 | XRF 1 | Zr KA1-HR-Tr | 8.47 % | 8.882 | 0.024 | 54.1 PPM | 0.58 mm |
| 0.0186 % | Sr | 38 | XRF 1 | Sr KA1-HR-Tr | 16.6 % | 3.807 | 0.019 | 33.0 PPM | 0.42 mm |

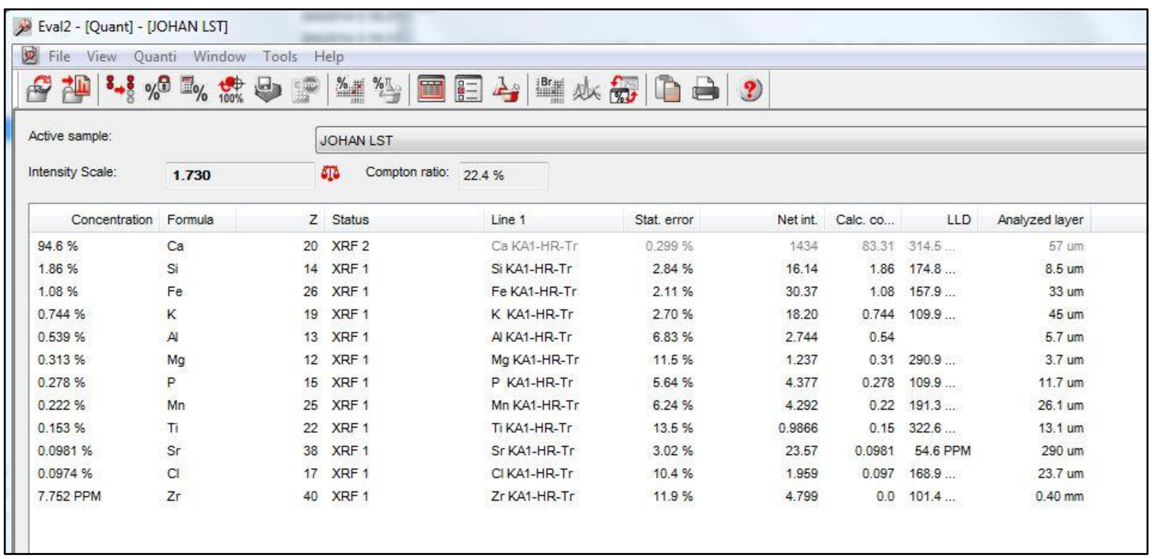

Eval2 - [Quant] - [JOHAN LST]

File View Quanti Window Tools Help

Active sample: JOHAN LST

Intensity Scale: 1.730 Compton ratio: 22.4 %

| Concentration | Formula | Z | Status | Line 1 | Stat. error | Net int. | Calc. co... | LLD | Analyzed layer |
|---|---|---|---|---|---|---|---|---|---|
| 94.6 % | Ca | 20 | XRF 2 | Ca KA1-HR-Tr | 0.299 % | 1434 | 83.31 | 314.5 ... | 57 um |
| 1.86 % | Si | 14 | XRF 1 | Si KA1-HR-Tr | 2.84 % | 16.14 | 1.86 | 174.8 ... | 8.5 um |
| 1.08 % | Fe | 26 | XRF 1 | Fe KA1-HR-Tr | 2.11 % | 30.37 | 1.08 | 157.9 ... | 33 um |
| 0.744 % | K | 19 | XRF 1 | K KA1-HR-Tr | 2.70 % | 18.20 | 0.744 | 109.9 ... | 45 um |
| 0.539 % | Al | 13 | XRF 1 | Al KA1-HR-Tr | 6.83 % | 2.744 | 0.54 | | 5.7 um |
| 0.313 % | Mg | 12 | XRF 1 | Mg KA1-HR-Tr | 11.5 % | 1.237 | 0.31 | 290.9 ... | 3.7 um |
| 0.278 % | P | 15 | XRF 1 | P KA1-HR-Tr | 5.64 % | 4.377 | 0.278 | 109.9 ... | 11.7 um |
| 0.222 % | Mn | 25 | XRF 1 | Mn KA1-HR-Tr | 6.24 % | 4.292 | 0.22 | 191.3 ... | 26.1 um |
| 0.153 % | Ti | 22 | XRF 1 | Ti KA1-HR-Tr | 13.5 % | 0.9866 | 0.15 | 322.6 ... | 13.1 um |
| 0.0981 % | Sr | 38 | XRF 1 | Sr KA1-HR-Tr | 3.02 % | 23.57 | 0.0981 | 54.6 PPM | 290 um |
| 0.0974 % | Cl | 17 | XRF 1 | Cl KA1-HR-Tr | 10.4 % | 1.959 | 0.097 | 168.9 ... | 23.7 um |
| 7.752 PPM | Zr | 40 | XRF 1 | Zr KA1-HR-Tr | 11.9 % | 4.799 | 0.0 | 101.4 ... | 0.40 mm |

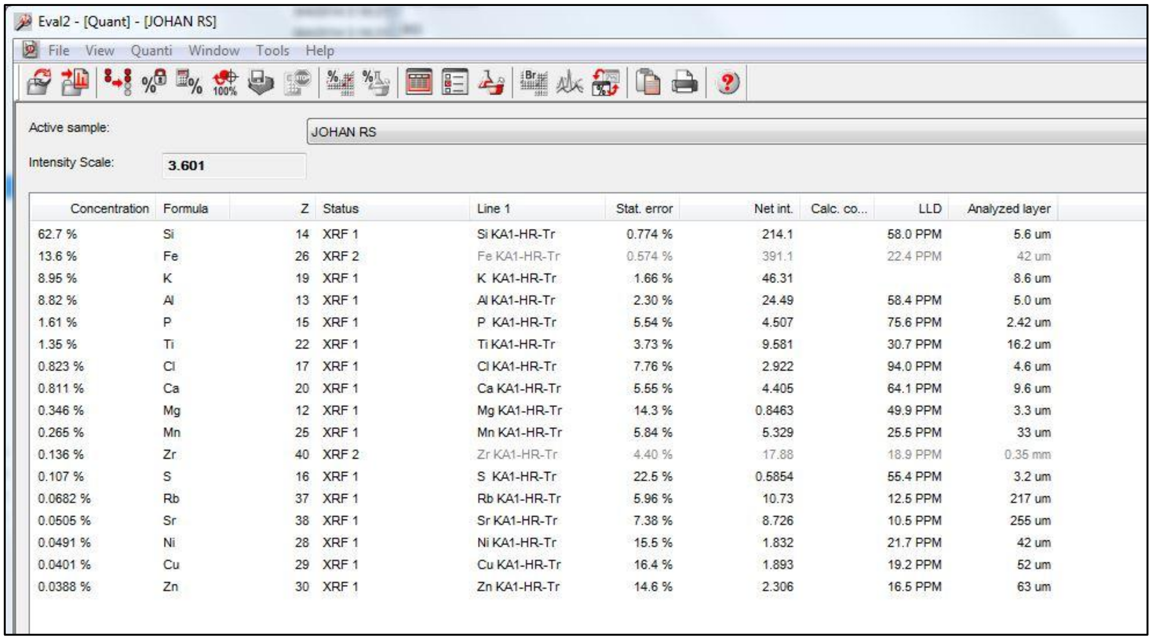

Eval2 - [Quant] - [JOHAN RS]

File View Quanti Window Tools Help

Active sample: JOHAN RS

Intensity Scale: 3.601

| Concentration | Formula | Z | Status | Line 1 | Stat. error | Net int. | Calc. co... | LLD | Analyzed layer |
|---|---|---|---|---|---|---|---|---|---|
| 62.7 % | Si | 14 | XRF 1 | Si KA1-HR-Tr | 0.774 % | 214.1 | | 58.0 PPM | 5.6 um |
| 13.6 % | Fe | 26 | XRF 2 | Fe KA1-HR-Tr | 0.574 % | 391.1 | | 22.4 PPM | 42 um |
| 8.95 % | K | 19 | XRF 1 | K KA1-HR-Tr | 1.66 % | 46.31 | | | 8.6 um |
| 8.82 % | Al | 13 | XRF 1 | Al KA1-HR-Tr | 2.30 % | 24.49 | | 58.4 PPM | 5.0 um |
| 1.61 % | P | 15 | XRF 1 | P KA1-HR-Tr | 5.54 % | 4.507 | | 75.6 PPM | 2.42 um |
| 1.35 % | Ti | 22 | XRF 1 | Ti KA1-HR-Tr | 3.73 % | 9.581 | | 30.7 PPM | 16.2 um |
| 0.823 % | Cl | 17 | XRF 1 | Cl KA1-HR-Tr | 7.76 % | 2.922 | | 94.0 PPM | 4.6 um |
| 0.811 % | Ca | 20 | XRF 1 | Ca KA1-HR-Tr | 5.55 % | 4.405 | | 64.1 PPM | 9.6 um |
| 0.346 % | Mg | 12 | XRF 1 | Mg KA1-HR-Tr | 14.3 % | 0.8463 | | 49.9 PPM | 3.3 um |
| 0.265 % | Mn | 25 | XRF 1 | Mn KA1-HR-Tr | 5.84 % | 5.329 | | 25.5 PPM | 33 um |
| 0.136 % | Zr | 40 | XRF 2 | Zr KA1-HR-Tr | 4.40 % | 17.88 | | 18.9 PPM | 0.35 mm |
| 0.107 % | S | 16 | XRF 1 | S KA1-HR-Tr | 22.5 % | 0.5854 | | 55.4 PPM | 3.2 um |
| 0.0682 % | Rb | 37 | XRF 1 | Rb KA1-HR-Tr | 5.96 % | 10.73 | | 12.5 PPM | 217 um |
| 0.0505 % | Sr | 38 | XRF 1 | Sr KA1-HR-Tr | 7.38 % | 8.726 | | 10.5 PPM | 255 um |
| 0.0491 % | Ni | 28 | XRF 1 | Ni KA1-HR-Tr | 15.5 % | 1.832 | | 21.7 PPM | 42 um |
| 0.0401 % | Cu | 29 | XRF 1 | Cu KA1-HR-Tr | 16.4 % | 1.893 | | 19.2 PPM | 52 um |
| 0.0388 % | Zn | 30 | XRF 1 | Zn KA1-HR-Tr | 14.6 % | 2.306 | | 16.5 PPM | 63 um |

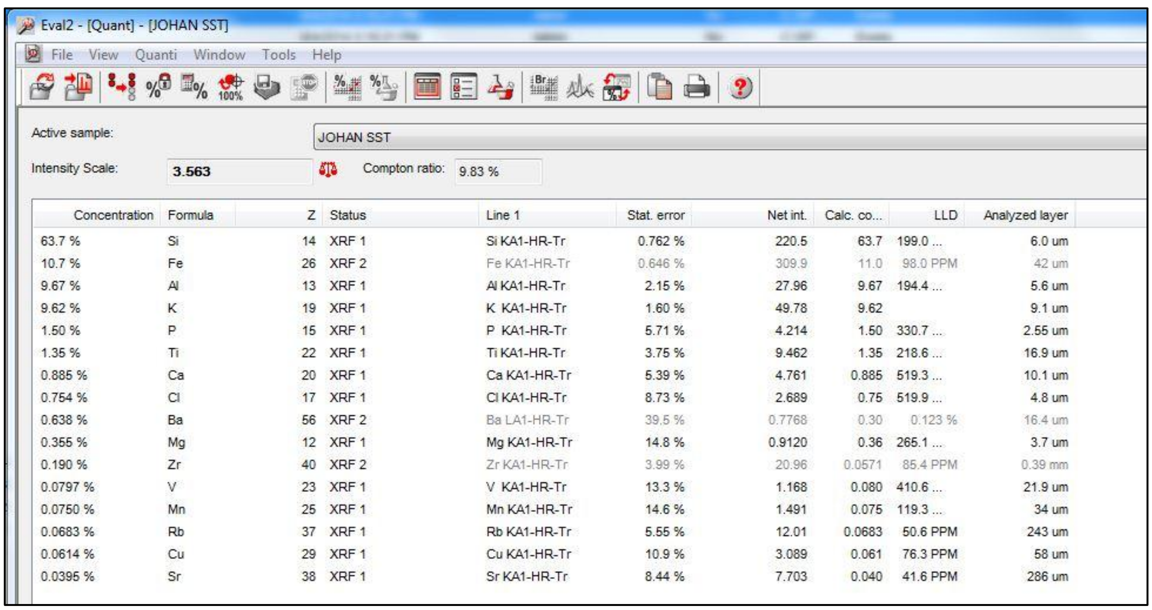

Eval2 - [Quant] - [JOHAN SST]

File View Quanti Window Tools Help

Active sample: JOHAN SST

Intensity Scale: 3.563 Compton ratio: 9.83 %

| Concentration | Formula | Z | Status | Line 1 | Stat. error | Net int. | Calc. co... | LLD | Analyzed layer |
|---|---|---|---|---|---|---|---|---|---|
| 63.7 % | Si | 14 | XRF 1 | Si KA1-HR-Tr | 0.762 % | 220.5 | 63.7 | 199.0 ... | 6.0 um |
| 10.7 % | Fe | 26 | XRF 2 | Fe KA1-HR-Tr | 0.646 % | 309.9 | 11.0 | 98.0 PPM | 42 um |
| 9.67 % | Al | 13 | XRF 1 | Al KA1-HR-Tr | 2.15 % | 27.96 | 9.67 | 194.4 ... | 5.6 um |
| 9.62 % | K | 19 | XRF 1 | K KA1-HR-Tr | 1.60 % | 49.78 | 9.62 | | 9.1 um |
| 1.50 % | P | 15 | XRF 1 | P KA1-HR-Tr | 5.71 % | 4.214 | 1.50 | 330.7 ... | 2.55 um |
| 1.35 % | Ti | 22 | XRF 1 | Ti KA1-HR-Tr | 3.75 % | 9.462 | 1.35 | 218.6 ... | 16.9 um |
| 0.885 % | Ca | 20 | XRF 1 | Ca KA1-HR-Tr | 5.39 % | 4.761 | 0.885 | 519.3 ... | 10.1 um |
| 0.754 % | Cl | 17 | XRF 1 | Cl KA1-HR-Tr | 8.73 % | 2.689 | 0.75 | 519.9 ... | 4.8 um |
| 0.638 % | Ba | 56 | XRF 2 | Ba LA1-HR-Tr | 39.5 % | 0.7768 | 0.30 | 0.123 % | 16.4 um |
| 0.355 % | Mg | 12 | XRF 1 | Mg KA1-HR-Tr | 14.8 % | 0.9120 | 0.36 | 265.1 ... | 3.7 um |
| 0.190 % | Zr | 40 | XRF 2 | Zr KA1-HR-Tr | 3.99 % | 20.96 | 0.0571 | 85.4 PPM | 0.39 mm |
| 0.0797 % | V | 23 | XRF 1 | V KA1-HR-Tr | 13.3 % | 1.168 | 0.080 | 410.6 ... | 21.9 um |
| 0.0750 % | Mn | 25 | XRF 1 | Mn KA1-HR-Tr | 14.6 % | 1.491 | 0.075 | 119.3 ... | 34 um |
| 0.0683 % | Rb | 37 | XRF 1 | Rb KA1-HR-Tr | 5.55 % | 12.01 | 0.0683 | 50.6 PPM | 243 um |
| 0.0614 % | Cu | 29 | XRF 1 | Cu KA1-HR-Tr | 10.9 % | 3.089 | 0.061 | 76.3 PPM | 58 um |
| 0.0395 % | Sr | 38 | XRF 1 | Sr KA1-HR-Tr | 8.44 % | 7.703 | 0.040 | 41.6 PPM | 286 um |

# APPENDIX B: Total Carbon Analysis Results

aj-Analyzer multi N/C 3100; multiWin 4.09; Serial No: N3-648/M

## AnalysisReport

| | | | |
|---|---|---|---|
| **Sample ID:** | BS_VDM | | |
| **Time of analysis:** | 16/7/2014 4:38:07 PM +0800 | **Method:** | TC_Solid |
| **User:** | Admin | **Sample quantity:** | 55.50mg |
| **Sample type:** | Sample | **Repetitions:** | 1 |
| **Status:** | Measurement completed successfully | **Furnace temperature:** | 1,200°C |

| | c | I eff | SD | CV | k0 | k1 | k2 | DF |
|---|---|---|---|---|---|---|---|---|
| TC | 9.91% | 8.55E5AU | | | 226.98 | 7.575E-3 | - | 0.82041 |

**Blank values**

| | | |
|---|---|---|
| TC | Boat blank | 7,576AU |

**Single replicates:**

| | Rep. | 1 |
|---|---|---|
| TC | c [%] | 9.91 |
| TC | I [AU] | 8.625E5 |

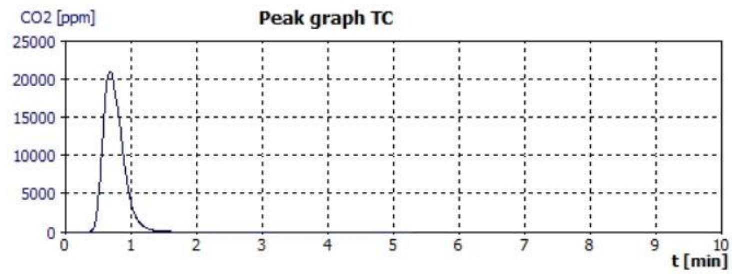


aj-Analyzer multi N/C 3100; multiWin 4.09; Serial No: N3-648/M

## AnalysisReport

| | | | |
|---|---|---|---|
| **Sample ID:** | BS_VDM(10%HCl) | | |
| **Time of analysis:** | 17/7/2014 3:56:55 PM +0800 | **Method:** | TC_Solid |
| **User:** | Admin | **Sample quantity:** | 55.50mg |
| **Sample type:** | Sample | **Repetitions:** | 1 |
| **Status:** | Measurement completed successfully | **Furnace temperature:** | 1,200°C |

| | c | I eff | SD | CV | k0 | k1 | k2 | DF |
|---|---|---|---|---|---|---|---|---|
| TC | 9.95% | 8.585E5AU | | | 226.98 | 7.575E-3 | - | 0.82041 |

**Blank values**

| | | |
|---|---|---|
| TC | Boat blank | 7,576AU |

**Single replicates:**

| | Rep. | 1 |
|---|---|---|
| TC | c [%] | 9.95 |
| TC | I [AU] | 8.66E5 |

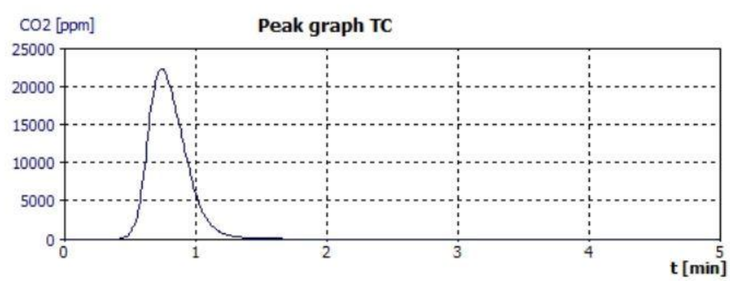

aj-Analyzer multi N/C 3100; multiWin 4.09; Serial No: N3-648/M

## AnalysisReport

**Sample ID:** GS_VDM

**Time of analysis:** 16/7/2014 4:44:46 PM +0800 | **Method:** TC_Solid

**User:** Admin | **Sample quantity:** 55.00mg

**Sample type:** Sample | **Repetitions:** 1

**Status:** Measurement completed successfully | **Furnace temperature:** 1,200°C

| | c | I eff | SD | CV | k0 | k1 | k2 | DF |
|---|---|---|---|---|---|---|---|---|
| TC | 0.952% | 6.379E4AU | | | 0 | 8.210E-3 | - | 1 |

**Blank values**

TC Boat blank 7,576AU

**Single replicates:**

| | Rep. | 1 |
|---|---|---|
| TC | c [%] | 0.952 |
| TC | I [AU] | 7.137E4 |

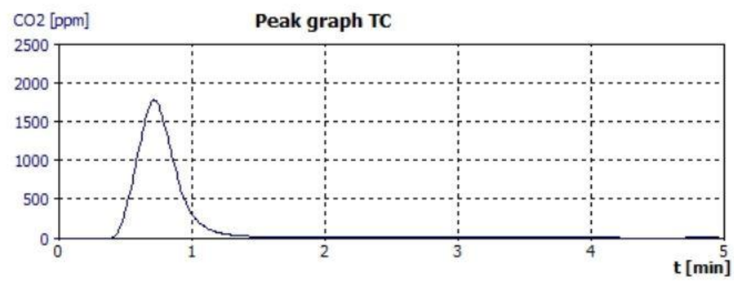


aj-Analyzer multi N/C 3100; multiWin 4.09; Serial No: N3-648/M

## AnalysisReport

**Sample ID:** GS_VPM(10%HCl)

**Time of analysis:** 17/7/2014 4:03:35 PM +0800 | **Method:** TC_Solid

**User:** Admin | **Sample quantity:** 55.10mg

**Sample type:** Sample | **Repetitions:** 1

**Status:** Measurement completed successfully | **Furnace temperature:** 1,200°C

| | c | I eff | SD | CV | k0 | k1 | k2 | DF |
|---|---|---|---|---|---|---|---|---|
| TC | 1.15% | 7.743E4AU | | | 0 | 8.210E-3 | - | 1 |

**Blank values**

TC Boat blank 7,576AU

**Single replicates:**

| | Rep. | 1 |
|---|---|---|
| TC | c [%] | 1.15 |
| TC | I [AU] | 8.5E4 |

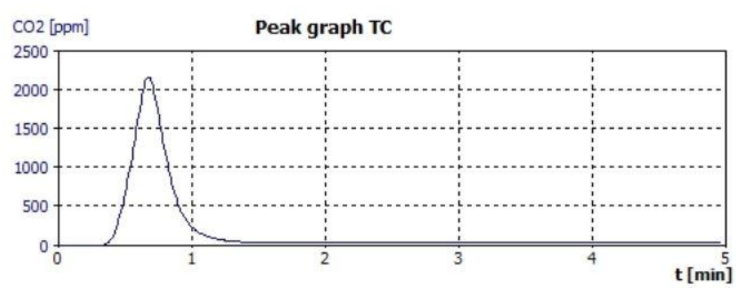

aj-Analyzer multi N/C 3100; multiWin 4.09; Serial No: N3-648/M

## AnalysisReport

**Sample ID:** LDM(10%HCl)

**Time of analysis:** 17/7/2014 3:40:04 PM +0800 **Method:** TC_Solid

**User:** Admin **Sample quantity:** 56.00mg

**Sample type:** Sample **Repetitions:** 1

**Status:** Measurement completed successfully **Furnace temperature:** 1,200°C

| | c | I eff | SD | CV | k0 | k1 | k2 | DF |
|---|---|---|---|---|---|---|---|---|
| TC | 1.32% | 9.023E4AU | | | 0 | 8.210E-3 | - | 1 |

**Blank values**

TC Boat blank 7,576AU

**Single replicates:**

| | Rep. | 1 |
|---|---|---|
| TC | c [%] | 1.32 |
| TC | I [AU] | 9.78E4 |

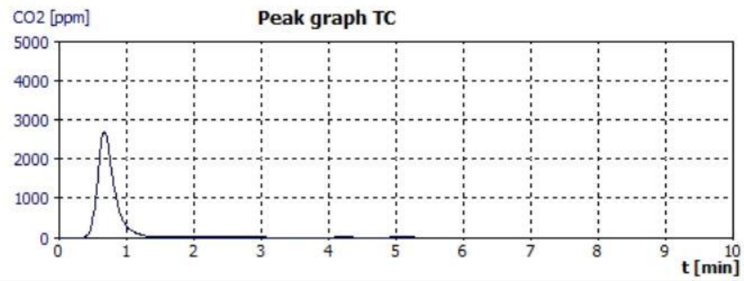


aj-Analyzer multi N/C 3100; multiWin 4.09; Serial No: N3-648/M

## AnalysisReport

**Sample ID:** LDM

**Time of analysis:** 16/7/2014 4:23:16 PM +0800 **Method:** TC_Solid

**User:** Admin **Sample quantity:** 56.00mg

**Sample type:** Sample **Repetitions:** 1

**Status:** Measurement completed successfully **Furnace temperature:** 1,200°C

| | c | I eff | SD | CV | k0 | k1 | k2 | DF |
|---|---|---|---|---|---|---|---|---|
| TC | 1.53% | 1.045E5AU | | | 0 | 8.210E-3 | - | 1 |

**Blank values**

TC Boat blank 7,576AU

**Single replicates:**

| | Rep. | 1 |
|---|---|---|
| TC | c [%] | 1.53 |
| TC | I [AU] | 1.121E5 |

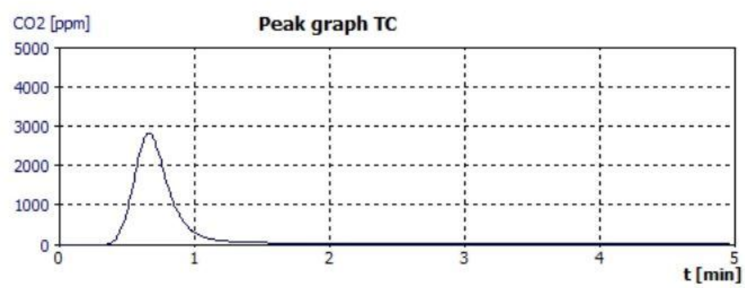

aj-Analyzer multi N/C 3100; multiWin 4.09; Serial No: N3-648/M

## AnalysisReport

**Sample ID:** RS_VDM

**Time of analysis:** 16/7/2014 4:31:27 PM +0800 **Method:** TC_Solid

**User:** Admin **Sample quantity:** 55.90mg

**Sample type:** Sample **Repetitions:** 1

**Status:** Measurement completed successfully **Furnace temperature:** 1,200°C

| | c | I eff | SD | CV | k0 | k1 | k2 | DF |
|---|---|---|---|---|---|---|---|---|
| TC | 0.313% | 2.134E4AU | | | 0 | 8.210E-3 | - | 1 |

**Blank values**

| | | |
|---|---|---|
| TC | Boat blank | 7,576AU |

**Single replicates:**

| | Rep. | 1 |
|---|---|---|
| TC | c [%] | 0.313 |
| TC | I [AU] | 2.892E4 |

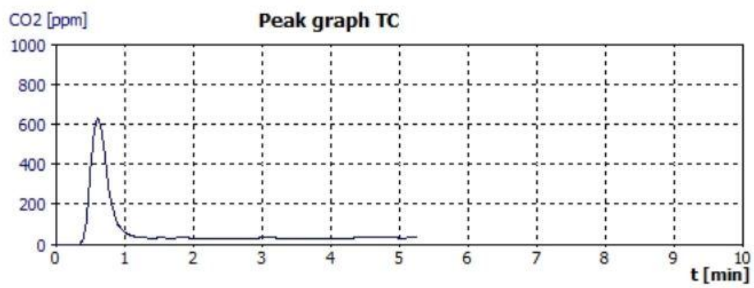


aj-Analyzer multi N/C 3100; multiWin 4.09; Serial No: N3-648/M

## AnalysisReport

**Sample ID:** RS_VDM(10%HCl)

**Time of analysis:** 17/7/2014 3:49:09 PM +0800 **Method:** TC_Solid

**User:** Admin **Sample quantity:** 55.90mg

**Sample type:** Sample **Repetitions:** 1

**Status:** Measurement completed successfully **Furnace temperature:** 1,200°C

| | c | I eff | SD | CV | k0 | k1 | k2 | DF |
|---|---|---|---|---|---|---|---|---|
| TC | 0.263% | 1.79E4AU | | | 0 | 8.210E-3 | - | 1 |

**Blank values**

| | | |
|---|---|---|
| TC | Boat blank | 7,576AU |

**Single replicates:**

| | Rep. | 1 |
|---|---|---|
| TC | c [%] | 0.263 |
| TC | I [AU] | 2.548E4 |

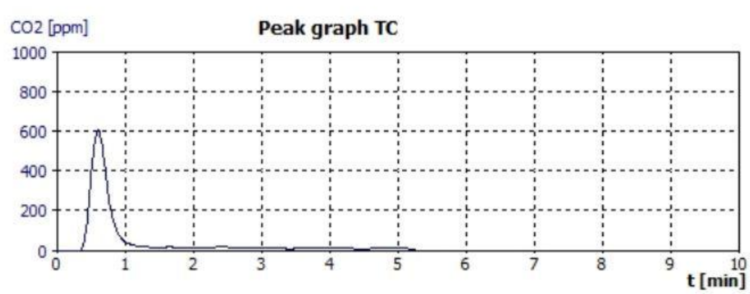

aj-Analyzer multi N/C 3100; multiWin 4.09; Serial No: N3-648/M

## AnalysisReport

**Sample ID:** SGA_SST
**Time of analysis:** 16/7/2014 4:15:48 PM +0800 **Method:** TC_Solid

**User:** Admin **Sample quantity:** 55.50mg
**Sample type:** Sample **Repetitions:** 1
**Status:** Measurement completed successfully **Furnace temperature:** 1,200°C

| | c | I eff | SD | CV | k0 | k1 | k2 | DF |
|---|---|---|---|---|---|---|---|---|
| TC | 0.265% | 1.793E4AU | | | 0 | 8.210E-3 | - | 1 |

**Blank values**

TC Boat blank 7,576AU

**Single replicates:**

| | Rep. | 1 |
|---|---|---|
| TC | c [%] | 0.265 |
| TC | I [AU] | 2.551E4 |

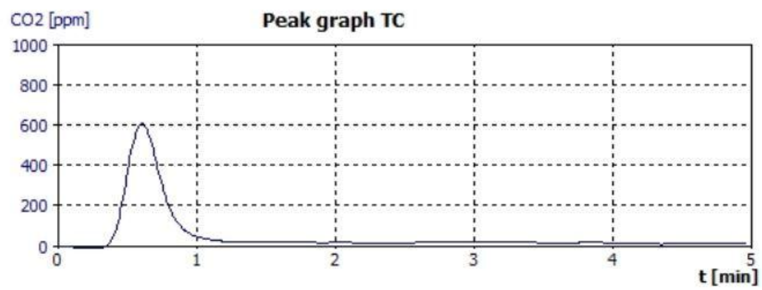


aj-Analyzer multi N/C 3100; multiWin 4.09; Serial No: N3-648/M

## AnalysisReport

**Sample ID:** SGA_SST(10%HCl)
**Time of analysis:** 17/7/2014 3:32:47 PM +0800 **Method:** TC_Solid

**User:** Admin **Sample quantity:** 55.50mg
**Sample type:** Sample **Repetitions:** 1
**Status:** Measurement completed successfully **Furnace temperature:** 1,200°C

| | c | I eff | SD | CV | k0 | k1 | k2 | DF |
|---|---|---|---|---|---|---|---|---|
| TC | 0.177% | 1.198E4AU | | | 0 | 8.210E-3 | - | 1 |

**Blank values**

TC Boat blank 7,576AU

**Single replicates:**

| | Rep. | 1 |
|---|---|---|
| TC | c [%] | 0.177 |
| TC | I [AU] | 1.955E4 |

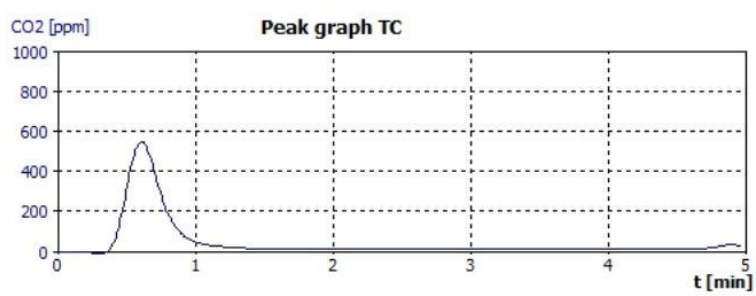

aj-Analyzer multi N/C 3100; multiWin 4.09; Serial No: N3-648/M

# AnalysisReport

**Sample ID:** STL_LST

| | | | |
|---|---|---|---|
| **Time of analysis:** | 16/7/2014 4:07:15 PM +0800 | **Method:** | TC_Solid |
| **User:** | Admin | **Sample quantity:** | 55.50mg |
| **Sample type:** | Sample | **Repetitions:** | 1 |
| **Status:** | Measurement completed successfully | **Furnace temperature:** | 1,200°C |

| | c | I eff | SD | CV | k0 | k1 | k2 | DF |
|---|---|---|---|---|---|---|---|---|
| TC | 11.0% | 9.512E5AU | | | 226.98 | 7.575E-3 | - | 0.82041 |

**Blank values**

TC Boat blank 7,576AU

**Single replicates:**

| | Rep. | 1 |
|---|---|---|
| TC | c [%] | 11.0 |
| TC | I [AU] | 9.588E5 |

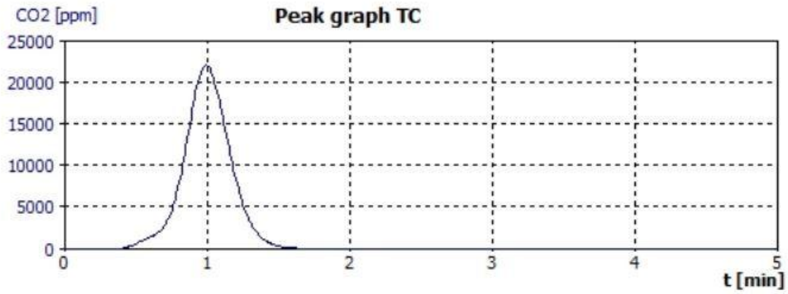


aj-Analyzer multi N/C 3100; multiWin 4.09; Serial No: N3-648/M

# AnalysisReport

**Sample ID:** STL_LST

| | | | |
|---|---|---|---|
| **Time of analysis:** | 17/7/2014 3:24:11 PM +0800 | **Method:** | TC_Solid |
| **User:** | Admin | **Sample quantity:** | 55.30mg |
| **Sample type:** | Sample | **Repetitions:** | 1 |
| **Status:** | Measurement completed successfully | **Furnace temperature:** | 1,200°C |

| | c | I eff | SD | CV | k0 | k1 | k2 | DF |
|---|---|---|---|---|---|---|---|---|
| TC | 2.12% | 1.426E5AU | | | 0 | 8.210E-3 | - | 1 |

**Blank values**

TC Boat blank 7,576AU

**Single replicates:**

| | Rep. | 1 |
|---|---|---|
| TC | c [%] | 2.12 |
| TC | I [AU] | 1.502E5 |

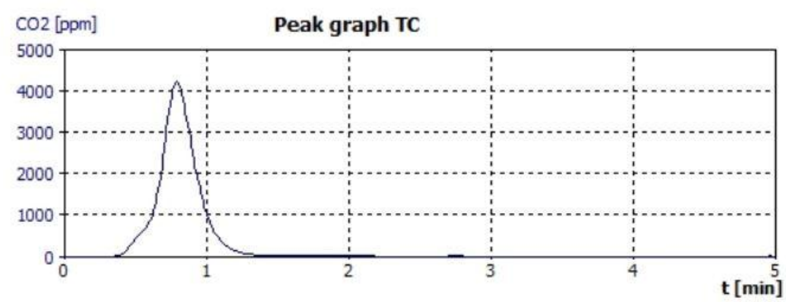

## APPENDIX C: Strike and Dip Data for Fractures in Teluk Mempelam

| Strike Direction ($^o$) | Dip Direction ($^o$) | Dip Angle ($^o$) | Strike Direction ($^o$) | Dip Direction ($^o$) | Dip Angle ($^o$) |
|---|---|---|---|---|---|
| 175 | 265 | 30 | 160 | 250 | 26 |
| 79 | 169 | 25 | 60 | 150 | 37 |
| 257 | 347 | 34 | 188 | 278 | 43 |
| 75 | 165 | 26 | 172 | 262 | 42 |
| 225 | 315 | 27 | 144 | 234 | 34 |
| 275 | 5 | 31 | 256 | 346 | 41 |
| 242 | 332 | 37 | 248 | 338 | 31 |
| 290 | 20 | 48 | 163 | 253 | 32 |
| 260 | 350 | 42 | 6 | 96 | 34 |
| 275 | 5 | 27 | 130 | 220 | 43 |
| 30 | 120 | 28 | 175 | 265 | 31 |
| 150 | 240 | 38 | 84 | 174 | 36 |
| 65 | 155 | 29 | 251 | 341 | 31 |
| 180 | 270 | 43 | 76 | 166 | 42 |
| 140 | 230 | 44 | 268 | 358 | 37 |
| 250 | 340 | 33 | 243 | 333 | 47 |
| 243 | 333 | 41 | 304 | 34 | 26 |
| 170 | 260 | 28 | 263 | 353 | 31 |
| 0 | 90 | 26 | 276 | 6 | 34 |
| 122 | 212 | 37 | 43 | 133 | 22 |
| 174 | 264 | 29 | 167 | 257 | 36 |
| 80 | 170 | 34 | 64 | 154 | 43 |
| 250 | 340 | 33 | 186 | 276 | 33 |
| 70 | 160 | 29 | 176 | 266 | 24 |
| 273 | 3 | 24 | 141 | 231 | 27 |
| 250 | 340 | 30 | 251 | 341 | 34 |
| 300 | 30 | 39 | 247 | 337 | 26 |
| 258 | 348 | 45 | 162 | 252 | 36 |
| 280 | 10 | 40 | 9 | 99 | 27 |
| 40 | 130 | 24 | 3 | 93 | 33 |